NASA CR-72100
TRW 06378-6007-R000

FOAM-IN-PLACE MATERIALS FOR HIGH VOLTAGE INSULATION IN A SPACE ENVIRONMENT

by

C. J. Holzbauer and R. J. Holbrook

prepared for

NATIONAL AERONAUTICS AND SPACE ADMINISTRATION

Contract NAS 3-8905

TRW SYSTEMS GROUP, TRW INC.
Redondo Beach, California

NASA CR-72100
TRW 06378-6007-R000

FINAL REPORT

FOAM-IN-PLACE MATERIALS FOR HIGH VOLTAGE INSULATION IN A SPACE ENVIRONMENT

by

C. J. Holzbauer and R. J. Holbrook

prepared for

NATIONAL AERONAUTICS AND SPACE ADMINISTRATION

April 1967

CONTRACT NAS 3-8905

Technical Management
NASA Lewis Research Center
Cleveland, Ohio
Space Technology Division
G. Gurski

TRW SYSTEMS GROUP, TRW INC.
One Space Park
Redondo Beach, California 90278

FOAM-IN-PLACE MATERIALS FOR HIGH VOLTAGE INSULATION IN A SPACE ENVIRONMENT

by

C. J. Holzbauer and R. J. Holbrook

ABSTRACT

Based on the results of thermal aging and dielectric strength screening tests, two foam-in-place materials were selected for extensive evaluation to determine their usefulness as high voltage insulation in space environments. These materials, CPR 23 and Stafoam AA-600, were subjected to an applied voltage of 10,000 VDC at 100°C for 3000 hours while exposed to a pressure of 10^{-5} torr or less. The permeability constant, ultraviolet radiation stability, vacuum weight loss and mechanical properties also were determined. Results of the tests indicate that these foams may be used as insulation for direct current high potentials in high vacuum environments at moderate temperature.

CONTENTS

SUMMARY

Material manufacturers and suppliers were surveyed to obtain data on available foam-in-place materials which might be useful as direct current high voltage insulation in spacecraft hardware. From an evaluation of these data, materials were selected for thermal aging, dimensional stability and dielectric strength testing. Also, during the specimen preparation for the tests, the processing characteristics of the materials were determined. Based on the results of these tests, two materials were selected for more extensive evaluation. These were CPR 23 Series, manufactured by the CPR Division of the Upjohn Company, and Stafoam AA-600 Series, a product of the Polytron Department of Olin-Mathieson Chemical Corporation. Both of these polyurethane materials were subjected to a series of tests to determine:

1) the effect of thermal vacuum and ultraviolet irradiation in vacuum on various electrical properties,
2) weight loss and gas permeability in vacuum,
3) mechanical properties, under both dynamic and static conditions, and
4) the thermal impedance in a vacuum.

Sixty specimens were subjected to an applied voltage of 10 KVDC while in a vacuum (10^{-5} torr or less) at 100°C for 3000 hours. A maximum of four specimens failed in this environment, three of the four being Stafoam AA-600 specimens.

Ultraviolet exposure at an intensity of the sun at one astronomical unit for 3000 hours at 100°C resulted in only minor changes in the dielectric constant and dissipation factor of the materials tested.

Moderate weight losses (varying from 1 to 4%) and weight loss rates were exhibited by the test materials. Considerable condensate was noted throughout the vacuum system following the 3000-hour high voltage vacuum test; however, it must be noted that there was approximately 21 pounds of foam in the chamber during this test.

In the dynamic testing, resonant frequency and amplification at resonant frequency as a function of density were determined. Values for both of these properties increased with increased density for both materials.

The Stafoam materials had higher compressive strength than did the CPR materials at the low (4 lb/ft^3) and high (20 lb/ft^3) densities while the CPR material had the higher compressive strength for the middle density (8 lb/ft^3). The compressive modulus of the Stafoam material was higher than that of the CPR material for all three densities tested.

Temperatures of 300°F or greater resulting from power dissipating components embedded in the foam materials caused permanent degradation of the foam.

I. INTRODUCTION

Currently there is considerable interest in foam-in-place materials as insulation for high voltage applications in space environments. The very substantial weight savings that may be realized by the use of these low density materials over the more conventional solid encapsulants makes the use of foams extremely desirable.

It is well known that entrapment of gas pockets and voids in solid insulation and the solution of gases in dielectric fluids degrade these insulation systems by contributing to corona formation and eventual failures of the insulation at voltages significantly lower than in the absence of gas entrapment. As a result, foam-in-place materials historically have been rejected as high voltage insulation materials.

With the advent of the space age and the attendant high cost of placing a payload into orbit, effort has been exerted to achieve smaller and lighter assemblies, and significant advances have been made in both the fields of components and packaging. Yet by far the greater mass of any assembly still is electrical insulation and the packaging materials. The functional portions of packages--the circuitry and circuit elements themselves--represent a small portion of the overall weight. As a result, it is necessary that lighter, lower density materials be considered for these packaging applications.

Two investigators, Dunaetz and Bahun[1], recognized the potential advantages of using low density cellular plastics as insulation for high voltage spacecraft applications. From their work, they concluded that rigid polyurethane foams could be used successfully in these applications. Theoretical and experimental efforts by Cuddihy and Moacanin[2] and Bunker[3], on the other hand, led these investigators to an opposite conclusion. As a result of the apparently conflicting conclusions resulting from these investigations and the still existing requirement to lighter insulation and packaging materials, this contract was initiated to provide further insight into the utility of foam-in-place materials as a high voltage space insulation.

II. CONCLUSIONS

1. Rigid foam-in-place polyurethanes are suitable for use in the space environment as direct current high voltage insulation materials at temperatures up to at least 100°C. Both materials evaluated in this program, CPR 23 Series and Stafoam AA-600 Series, appear adequate to insulate direct current voltages up to at least 5000 volts.

2. Ultraviolet radiation approximating solar intensity did not produce any significant effect on either electrical or physical properties of the materials.

3. Analytical methods can be used to predict reasonably well the behavior of these materials under dynamic loading.

4. The resonant frequency and amplification at resonant frequency of the materials tested increase with increasing density.

5. Because of the high exotherm generated by foam-in-place materials, consideration should be given to the temperature capability of the components embedded in these materials. Limiting the volume to be foamed is one means of restricting the exotherm.

6. For a given foam material, the higher density products generally exhibit a slower exothermic temperature rise than do their lower density counterparts. Furthermore, Freon blown foams produce lower exothermic temperatures than do the carbon dioxide blown materials.

7. Because of the low thermal conductivity of these materials, the power dissipation of embedded components must be one of the prime considerations in foam encapsulated module design. Temperatures above 300°F cause permanent physical damage to these foam materials.

III. GENERAL DISCUSSION

Foam-in-place materials have only recently begun to receive serious consideration for application in spacecraft high voltage equipment. The principal reason for deleting these materials from consideration in the past is because their dielectric strength and corona initial voltages are lower than solid dielectric materials. In high voltage applications when using foamed (cellular) materials, there are three important conditions favorable to corona formation. These are high electric field, non-uniform electric field, and the presence of a gas. Since a large volume of the foam material is a gas, the dielectric strength of the gas should contribute, perhaps significantly, to the dielectric strength of the foam. In a vacuum environment, the permeability rate of the gas through the foam will determine the pressure of the gas in the foam cell at any time. Since the dielectric strength of the gas is proportional to its pressure, a decrease in gas pressure within the foam cell may result in decreased dielectric strength of the foam. Of particular interest is the dielectric strength of the foam materials when the pressure of the gas in the cell approaches that at which its dielectric strength is minimal (Paschen's minimum). An experiment was included in this program to determine the effect of prolonged vacuum exposure on the dielectric strength of the foam.

Although the electrical properties are the primary consideration in this test program, other important properties also were investigated. One of these is the dimensional stability of the materials over the anticipated environmental temperature extremes. Since the foam is used to encapsulate fragile electronic components and devices, expansion or contraction of the foam may create stresses which could lead to mechanical failure of the embedded components. In solid dielectric and encapsulating materials, the expansion and contraction of the materials is described principally by the thermal coefficient of linear expansion. However, in foam materials, an additional source of stress results from the increase of pressure with increase in temperature of the gas within the foam cells. This source of stress probably is not significant at low and moderate temperatures because the foam is structurally adequate to withstand the pressures at these temperatures. However, at high temperatures the foam material weakens while the pressure within the foam cells increases, thereby increasing the probability of dimensional instability.

Since the foam must provide structural support as well as electrical insulation for the embedded components, the mechanical properties of the foams were also determined. The determinations were made under conditions of both static and dynamic loading.

Finally, since it was anticipated that applications will arise where the foam may be subjected directly to ultraviolet irradiation, a test was included to determine the effect of irradiation in the .25 to .4 micron range on the dielectric constant and dissipation factor of the materials.

This contract was carried out essentially in two phases. In the first phase of the contract, the initial effort was directed toward a survey of vendor literature to determine available foam materials and their reported properties. From the results of this survey, nine series of compounds were selected for the first screening test, thermal aging. Materials which successfully passed the thermal aging test were tested for their dielectric strength and corona initiation voltage. From these data, the two most promising materials were selected for the more extensive final evaluation tests.

In the second phase, the testing of the two selected materials consisted of the following tests:

a. Gas Permeability Rate Test
b. High Temperature, Vacuum, Corona Initiation and Breakdown Voltage Test
c. Vibration Characteristics Test
d. Compressive Properties Test
e. Vacuum Weight Loss and Weight Loss Rate Test
f. Ultraviolet Radiation Stability Test
g. Thermal Test

IV. EVALUATION AND RESULTS

A. Preliminary Screening

1. Literature Survey

Seventeen manufacturers responded to the request for their literature supplying data on fifty-seven series of foam-in-place materials of six basic types; polyurethane, epoxy, silicone, phenolic, polyethylene and polystyrene.

The foam property data received from the manufacturers are presented in summary form in Table I. Table II identifies the manufacturers of the foam product.

In accordance with the terms of the Contract, materials most nearly meeting Contract specified requirements would be subjected to the preliminary screening tests. The requirements specified by the Contract are listed in Table III. Comparing the manufacturers' reported data with these requirements, nine materials were selected for test. The nine materials, with other pertinent data including mix ratios and cure schedules, are presented in Table IV. The nine compounds include eight polyurethanes and one epoxy. Selection of the nine compounds, although based on their ability to meet the NASA specified requirements, was nevertheless rather arbitrary in that so few data were available from most manufacturers. Furthermore, the properties reported varied among the manufacturers. The significance of the reported data also is often questionable, i.e., some manufacturers report specification values, others report typical values, and still others report values obtainable only under ideal conditions.

The CPR 200 Series and Nopcofoam BX-249 were selected primarily because they are halogenated hydrocarbon (Freon*) blown systems, as opposed to the majority of the materials which are carbon dioxide blown. The purpose for including these was to obtain a comparison of the thermal and electrical characteristics of Freon and carbon dioxide blown systems.

---

*Trade name of E. I. DuPont de Nemours and Company

The Eccofoam EFF, a one component epoxy powder, was selected to obtain comparative data for an epoxy foam.

The remaining materials, CPR 23 and 727 Series, Eccofoam FPH Series, Nopcofoam G-300 Series, and Stafoam 100 and AA-600 Series, were selected because of their general conformance to the specified requirements.

2. Thermal Aging

a. Discussion

The Thermal Aging Test was the first screening test performed. The purpose of this test was to determine the dimensional stability and gross weight loss of the nine selected foam materials.

b. Experimental

For each foam material and density, two specimen configurations were utilized. One configuration was a rectangular parallelepiped, 10 x 5 x 4 inches with all six faces of the foam exposed. Molds for this configuration were made of one-quarter inch aluminum (6061) plates, bolted together, cleaned, and coated with a fluorocarbon mold release. The second configuration was also a rectangular parallelepiped, but the foam was poured into an aluminum (6061) container which became a permanent part of the specimen. This resulted in a specimen with five sides enclosed and only one side exposed. The outside dimensions of the aluminum can were 10.5 x 5 x 4 inches with a nominal wall thickness of .08 inch. Prior to foaming the specimens, the aluminum cans were prepared using the standard sulfuric acid-sodium dichromate etch to insure good adhesion of the foam to the container walls. Figure 1 is a photograph of the two specimen configurations.

For both configurations, the molds were preheated to 40-45°C before pouring in the foam-in-place materials. The foam-in-place materials were proportioned in accordance with the manufacturer's recommendations. Material proportions and cure schedules for each material are presented in Table IV.

During specimen preparation, a thermocouple was located in the approximate center of the aluminum container to monitor the exothermic temperature of the foaming reaction.

The initial specimen weight and physical dimensions were determined and recorded.

The specimens were subjected to the following thermal environments:

(a) From room ambient temperature (22°C), the temperature of the specimens was raised to 125°C in 6 hours and maintained for 10 hours.

(b) The temperature of the specimens was lowered to 22°C in 5 hours and maintained for 3 hours.

(c) Steps (a) and (b) were repeated four times for a total of five thermal cycles from 22°C to 125°C and back to 22°C.

(d) The temperature of the specimens was raised to 125°C in 6 hours and maintained for 210 hours.

(e) The temperature of the specimens was lowered to room temperature.

Following the thermal aging, the weight and physical dimensions of each specimen were determined. The change in weight and dimensions for each specimen was calculated.

c. Results

Of the nine compounds selected for thermal aging testing, three were immediately determined to be unsuitable for evaluation based on their handling and foaming characteristics. These materials were the CPR 200 Series, the Stafoam 100 Series, and Eccofoam EFF. The specimens prepared from the CPR 200 Series materials, a Freon blown system, all resulted in incomplete filling of the molds and products with densities ranging from 20 to 50 lb/ft^3. The Stafoam 100 Series materials, a CO_2 blown system, also resulted in incomplete filling of the molds and specimen densities approximately twice those reported by the vendor. The Eccofoam EFF, a one component epoxy powder, resulted in products that were non-uniform in density and severely stress cracked. In all three cases, additional material was ordered from each vendor and new specimens prepared. However, the same results were obtained. Consequently, these three materials were removed from the test plan.

The results of thermally aging the remaining six materials are presented in Table V. The Nopcofoam BX-249 Series, a Freon blown system, exhibited weight and dimensional changes greater than three percent while the five remaining materials suffered smaller changes and generally appeared to be comparable in both weight and dimensional stability.

The exothermic temperature rise of the materials found suitable for thermal aging are presented in Figure 2. All the materials tested exhibited exothermic temperatures varying from 134°C to 204°C. The lowest exothermic temperature, approximately 134°C, resulted from the Nopcofoam BX-249 Series while the highest temperatures, 194°C to 204°C, were exhibited by the Stafoam AA-600

Series. Although no general conclusions can be drawn from the data regarding the relationship of exotherm temperature to density, such a relationship can be deduced for each particular material. Generally, it was found that for a given material the higher density product exhibited a slower exothermic temperature rise than did its lower density counterpart. Furthermore, it is noted that the lowest exothermic temperatures were produced by the Freon blown system (BX-249). Because of the high exotherm generated by foam-in-place materials, special consideration should be given to the temperature capability of the components embedded in these materials and every attempt should be made to limit the foaming volume to assist in restricting this temperature rise.

3. Dielectric Characteristics Test

a. Discussion

An electric field applied across a dielectric compound is capable of producing several phenomena within the compound, depending on the nature of the field intensity. Two of these phenomena produced by intensified electric fields are the corona or emission discharge and electrical breakdown. The corona discharge is an intermittent discharge of varying frequency and of generally low current, while breakdown is a continuous discharge capable of conducting a large current. The corona discharge is generally produced at potentials lower than those considered necessary for breakdown. It is probable that the corona discharge mechanism functions to produce the breakdown condition within the compound through a process of physical/chemical reactions, and that these reaction rates are dependent upon the applied potential. Hence, a breakdown condition may be achieved at the potential at which corona discharge begins, but the time to breakdown will be greater than would be obtained if the potential were continually increased at a given rate.

The effects of corona discharge and breakdown within a compound will depend on the nature of the products formed by the reaction, the extent of the reaction and the reversibility of the reaction. For many gaseous compounds, the corona discharge and breakdown have no permanent effects upon the reactants; when the applied potential is reduced to below the discharge level, the compound is returned to its original form. The reaction of solid compounds in an electrical discharge, however, is usually non-reversible. For example, hydrocarbons of the $-CH_2-$ type may be reduced or oxidized irreversibly in an electrical discharge, as follows:

$$-CH_2- \longrightarrow \underline{C} + H_2 \text{ (reduction)}$$

$$-CH_2- \xrightarrow{3(O)} CO_2 + H_2O \text{ (oxidation)}$$

With the irreversible process, the type and quantity of products resulting are the primary consideration. When such products are conductive or significantly inferior electrically to the material from which they were formed, the material may be no longer useful as a dielectric.

The corona discharge and breakdown phenomena can be produced in all dielectric compounds--solids, liquids and gases. Each compound has a potential at which these phenomena occur, which is related to the conditions of the determination. It can be stated that with the exception of gases at the extremes of high and low pressure, gases exhibit lower corona discharge and breakdown potential than do liquids or solids. The general order of reactivity is:

$$\text{Increasing Discharge Potential (Voltage)} \;\; \Bigg\uparrow \begin{array}{l}\text{Solids}\\ \text{Liquids}\\ \text{Gases}\end{array}$$

The study of corona discharge and breakdown within cellular compounds is a new avenue of exploration. Cellular compounds (or foam dielectrics), for the purpose of analysis, are considered as composites consisting of a solid dielectric and a gas. The solid dielectric forms the cell wall or membrane, while the gas occupies the volume between the interconnected membranes.

The behavior of these compounds in an electric field is predicted to be functionally dependent on both the gas and the solid dielectric, including any reactions between the two as a result of the applied potential. Because of the lower discharge potential of gases, the discharge potential for the cellular compounds is presumed to be dependent on the relative quantities of the solid and the gas, hence, on the density of the compound. Another parameter which should affect the discharge potential is the pressure of the cell gas. As this pressure is increased the discharge potential will increase, and for pressure reductions there will be a corresponding decrease in the discharge potential.

Additional factors which influence the corona discharge and breakdown for cellular compounds are the frequency of the applied potential, the electrode geometry, the electrode polarity, the electrode spacing, and the rate of potential increase. A knowledge of these parameters and their relationships is necessary to understand and to predict the behavior of these compounds when they are subjected to high electric fields.

b. Experimental

The specimen and electrode configurations for these experiments are shown in Figure 3. The configuration consisted of an embedded electrode pair contained in a four-inch cube (64 in^3) of the compound. The electrodes were of the point-plane type; the plane was a one-inch square plate, and the point a rod of one-eighth (1/8) inch diameter with a hemispherical end. Both electrodes were brass, procured to Federal Specification QQ-B-626, Composition 22.

The specimens for analysis were prepared by mixing the compound reactants in accordance with the manufacturer's instructions, and then pouring measured amounts into closed cavity molds containing the pre-spaced electrode pairs. The molds had been pre-heated to 40-50°C. The cure cycles for the compounds were as specified in Table IV. The cured specimens were returned to room temperature for testing.

The test circuit for determining the corona discharge and breakdown potentials is shown in Figure 4. The apparatus consisted of a high voltage, direct current power supply (Kilovolt Corp. Model KV120-5S) which was connected to the specimen by a high voltage, shielded cable. The specimen was contained in a shielded high voltage chamber, and was, in turn, connected to the corona discharge detector. The detector consisted of a resistor in series with the specimen and voltage measuring device (Tektronix Oscilloscope Model 545 or 585, using a Type W pre-amp) for recording the voltage drop across the resistor. In addition, a Zener diode was placed across the resistor to limit the voltage across the pre-amp to 6 volts. Using a 10^6 ohm resistor, corona discharge currents as low as 10^{-9} amperes can be detected by this method.

The test specimen was placed in the shielded chamber and connected to the high voltage lead and to the detector circuit. Voltage was then applied to the specimen and increased at a rate of approximately 50 volts per second until corona discharge was observed on the oscilloscope. Discharge was considered to be occurring when 10^{-8} to 10^{-7} ampere currents were observed. Upon detection of corona discharge, the voltage was held constant for one to two minutes and the magnitude and frequency of the discharge were observed. Then, the voltage was increased until breakdown occurred.

For those experiments where the time to failure was to be determined, the voltage was held constant at the discharge potential. The time, the discharge currents and the discharge frequency were then monitored until the specimen failed or was removed in order to examine the discharge effects.

For each specimen the following observations were made and recorded: the corona discharge potential and the magnitude of the corona current; the breakdown potential; time to failure (when applicable); electrode spacing and polarity; and the nature of the breakdown.

c. Results

The experimental results are divided into two main areas. The first one deals with an analysis of the discharge phenomena and the other gives a comparative evaluation of the discharge and breakdown potentials for different cellular compounds.

The corona discharge analysis was conducted using Eccofoam FPH at densities of 4 and 22 pounds per cubic foot (lb/ft^3) identified as FPH12-4H and FPH12-10H, respectively. The results of these tests are summarized in Tables VI and VII. Table VI contains the discharge and breakdown data for the FPH12-4H (4 lbs/ft^3) at 50 and 250 mil electrode spacings, and for the FPH12-10H (22 lb/ft^3) covering electrode spacing from 50 to 250 mils.

The FPH12-4H with a 50 mil spacing exhibited an average breakdown potential of 10.5 KVDC while the FPH12-10H had an average breakdown potential of 59 KVDC. When the spacing was increased to 250 mils, the FPH12-4H broke down at 46 KVDC (average), while the average breakdown of the FPH12-10H was 73 KVDC. With the exception of the 50 mil spacings, the corona discharge potentials for the FPH12-4H were in the range observed for the FPH12-10H, i.e., approximately 20 to 40 KVDC.

A comparison of the corona discharge and breakdown potentials as a function of electrode spacing are presented in Figures 5 and 6. These results indicate that for the lower compound densities both the discharge and breakdown potentials are dependent on the electrode spacing. At the higher density the discharge potential appears to be nearly independent of the electrode spacing.

Table VII presents the time-to-failure data for both the FPH12-4H (4 lb/ft^3) and the FPH12-10H (22 lb/ft^3). The electrode spacing for these specimens was 1000 mils (1 inch). Both densities produced corona discharges at approximately 70 KVDC. The potential on the FPH12-4H was increased to 80 KVDC, and after 30 minutes at this potential the specimen failed. The potential on the FPH12-10H was increased to 82 KVDC; after 15 minutes at this potential the corona discharge currents had increased to 10^{-7} amperes, and the test discontinued. Dissection of the specimen showed a carbonaceous path emanating from the point (or ground) electrode. The length of the path was approximately one-quarter (1/4) of an inch.

These corona discharge and breakdown tests produced two general types of failures. The predominant failure mode was the production of a carbonaceous residue of low resistance (less than 10^5 ohms). Less frequently observed was the apparent vaporization of the compound, leaving a void in the area of the electrodes but no carbonaceous products; with this type of failure the resistance was extremely high, greater than 10^{10} ohms.

An additional parameter which was observed during the analyses was the effects of electrode polarity. The data (Table VI) indicate that neither the corona discharge nor the breakdown potentials are influenced by the electrode polarity.

Table VIII summarizes the results of the discharge and breakdown tests for the six compounds evaluated. The electrode spacings for all specimens were 125 mils and in all cases the point electrode was at ground potential. Compound densities of 4, 8, and 20 lbs/ft^3 (nominal) were used in each analysis. The breakdown potentials range from 17.5 KVDC for the CPR 727-8 (minimum for all compounds) to 64 KVDC for both the FPH12-10H and the Nopcofoam BX 249-6.

The corona discharge potentials ranged from 17.5 KVDC (CPR 727-8) to 48 KVDC (BX 249-6). It is noted that the two Freon blown compounds, BX 249-N and BX 249-6, produced discharge potentials greater than those of the carbon dioxide (CO_2) blown compounds. The CO_2 blown compounds have discharge potentials ranging between 17.5 and 38 KVDC which correspond to the 20 to 40 KVDC discharge values observed in the previously discussed corona analysis.

These data seem to indicate that the breakdown potential may be proportional to the log of the compound density, although there is insufficient data to conclusively confirm this hypothesis.

B. Final Evaluation

Two materials were selected for final evaluation based on the results of their general processing characteristics and the results of the preliminary screening tests. Since polyurethane foam materials generally exhibit very short pot lives or working times, this processing characteristic was given strong consideration in the selection of the two materials. Selected for final evaluation were the CPR 23 Series and the Stafoam AA-600 Series foams.

1. Permeability

a. Discussion

Since a portion of the dielectric strength of a foam material is attributable to the gas within the foam cells, and since the dielectric strength of a gas is a function of the gas pressure, information relating to the permeability of the gas through the foam is of value in determining the usefulness of the foam as an electrical insulation in low pressure environments.

The general expression for the permeability of a gas through a membrane is given by

$$\frac{dw}{dt} = \frac{K_p A P}{L} \qquad ①$$

where w = weight of gas
t = time
A = area of membrane
P = pressure difference across membrane
L = thickness of membrane
Kp = permeability constant

From the ideal gas law

$$w = \frac{PV\ MW}{RT} \tag{\textcircled{2}}$$

where P = pressure
V = volume of gas
MW = molecular weight
R = gas constant
T = temperature

In the experimental approach used to determine the data necessary to calculate the permeability constant (Kp), the pressure of the gas was measured using a mercury manometer. As a result, a pressure change in the gas was accompanied by a slight volume change. Differentiating ② with respect to time defines these relationships and yields

$$\frac{dw}{dt} = \frac{MW\ d(PV)}{RT\ dt} \tag{\textcircled{3}}$$

Combining ① and ③ and rearranging yields

$$\frac{Kp\ A\ RT}{L\ MW}\,dt = \frac{V}{P}\,dP + dV \tag{\textcircled{4}}$$

Since, for constant temperature, the plot of pressure with respect to volume is a straight line, i.e., the pressure is directly proportional to the volume of gas,

$$V = \left(\frac{Vo - V}{Po - P}\right)P + b \tag{\textcircled{5}}$$

where V = volume at any time t
Vo = volume at time zero (o)
P = pressure at any time t
Po = pressure at time o
b = constant (intercept of V axis, defines volume of gas when pressure = o)

To determine the permeability constant (Kp) for each of the test materials using Equation ④ , experimental data is substituted into Equation ⑤ , from which an expression for volume V is obtained.

This is then substituted into Equation ④ .

From Equation ⑤

$$V = a P + b$$ ⑥

$$\text{where } a = \frac{Vo - V}{Po - P}$$ ⑦

Substituting the value of V from Equation ⑥ into Equation ④ yields

$$c_1 \, dt = dV + (a + \frac{b}{P}) \, dP$$ ⑧

$$\text{where } c_1 = \frac{Kp \; A \; R \; T}{L \; MW}$$ ⑨

Integrating ⑧ yields

$$c_1 t = V + aP + b \ln P + C_2$$ ⑩

Substituting Equation ⑥ for V in Equation ⑩ yields

$$c_1 t + 2aP + b + b \ln P + C_2$$ ⑪

but when $t = o$,

$P = Po$

therefore, $C_2 = -(2aPo + b + b \ln Po)$

Equation ⑪ now reduces to

$$c_1 t = 2a(P-Po) + b \; (\ln \frac{P}{Po})$$ ⑫

Replacing the expression for C_1 from ⑧ and solving ⑫ for the permeability constant Kp yields

$$Kp = \frac{L \; MW \left[2a(P-Po) + b \; (\ln \frac{P}{Po}) \right]}{t \; ART}$$ ⑬

b. Experimental

Figure 7 shows a photograph of the apparatus used in the gas permeability experiment. Figure 8 is a schematic view of one of the experimental set-ups showing its essential features. The foam test specimens were prepared from a large block of the foam which had been foamed and cured as described in Table IV. The test specimens were then machined to a disk configuration, 3 inches in diameter by one-half inch thick. The resulting specimen consequently had no skin on any surface. The circumferential area of the specimen was painted with an epoxy-polyamide resin system* and allowed to cure overnight. The specimen was then bonded into the bell jar using the same adhesive formulation. A porous sintered glass disk** was then bonded with the same adhesive into the bell jar immediately adjacent to the specimen. This disk was used to support the foam specimen to prevent distortion and/or failure of the specimen during the testing as a result of the pressure differential. The adhesive was cured for a minimum of 7 days at room temperature before testing commenced.

The bell jar containing the specimen was fused to a mercury manometer. The volume of air in the manometer side of the apparatus was evacuated with a mechanical vacuum pump and backfilled to ambient pressure with dry nitrogen. The side arm used for this operation was then fused closed, so that the nitrogen was now in a totally enclosed glass system with the only means of entry or escape of gas being through the foam specimen. The bell jar was seated on a vacuum base plate and then evacuated using an oil diffusion pump and a mechanical forepump. Pressure on this side of the specimen was maintained at 10^{-4} mm Hg or below during the entire test period of 3000 hours.

The pressure of the enclosed gas volume was monitored periodically throughout the test.

* Epon 828 (Shell Chemical Co.)	35	parts by weight
Versamid 140 (General Mills)	65	parts by weight

** Model 7176, Porosity E, Ace Glass Co., Wineland, N. J.

c. Results

Table IX reports the pressures of the enclosed gas volumes behind the specimens at various times throughout the test, while Figure 9 is the graphical presentation of these experimental data. The slope of the resulting plot was used to calculate the permeability constant (Kp). It may be noted that for all the materials tested except CPR 23-20, the rate of pressure decrease was initially higher than the final value; i.e., the slope of the curve for the first few hundred hours was greater and it decreased gradually to its final value. If the pressure in the foam cells was at or near atmospheric pressure at the time the test was initiated, an opposite result should have been obtained. However, these results would have been anticipated if the pressure within the foam cells initially was less than atmospheric. No further explanation for this apparent anomaly is postulated.

Using Equation ⑬, the permeability constant (Kp) for each of the six test materials was calculated and is presented below.

Stafoam 604: $Kp = 7.3 \times 10^{-13}$ $g.cm.cm^{-2}.sec^{-1}.cm\ Hg^{-1}$

Stafoam 608: $Kp = 6.8 \times 10^{-13}$ $g.cm.cm^{-2}.sec^{-1}.cm\ Hg^{-1}$

Stafoam 620: $Kp = 4.9 \times 10^{-13}$ $g.cm.cm^{-2}.sec^{-1}.cm\ Hg^{-1}$

CPR 23-4 : $Kp = 4.4 \times 10^{-13}$ $g.cm.cm^{-2}.sec^{-1}.cm\ Hg^{-1}$

CPR 23-8 : $Kp = 5.3 \times 10^{-13}$ $g.cm.cm^{-2}.sec^{-1}.cm\ Hg^{-1}$

CPR 23-20 : $Kp = 4.8 \times 10^{-13}$ $g.cm.cm^{-2}.sec^{-1}.cm\ Hg^{-1}$

2. Vacuum - Dielectric Test

a. Discussion

Cellular compounds when subjected to conditions of high temperature and high vacuum are predicted to display two opposing phenomena. First, as a result of the increased temperature there will be a proportional increase in the pressure of the cell gas. Second, when subjected to vacuum conditions the gas within the cell will diffuse out of the cell in an effort to equalize the internal and external pressures. This diffusion process results in a decrease in the cell gas pressure. Temperature also affects the diffusion process, an increase in temperature resulting in an increase in the cell membrane permeability and hence in a greater diffusion rate. Further, the temperature as it affects the gas pressure is related to the diffusion phenomena, since the permeability rate is a function of the pressure difference across the membrane. The net effect of subjecting a cellular compound to conditions of increased temperature and reduced pressure is predicted to be an initial increase in the cell gas pressure which gradually reduces until an equilibrium pressure with the external environment is achieved.

The discharge and breakdown potentials for cellular compounds when subjected to conditions of increased temperature and reduced pressure are expected to be dependent upon the pressure effects resulting from these conditions. The initial effect would be an increase in both the discharge and breakdown potentials corresponding to the increased pressure of the cell gas. As the cell gas diffuses producing reduced pressures, the discharge and breakdown potentials would be reduced until a minimum potential condition is achieved, analogous to Paschen's critical minimum.

At this point, the discharge potential would begin to increase for any subsequent reduction in pressure. It is noted that the possible increase in discharge and breakdown potentials resulting from the increased pressure caused by increased temperature may be all or partially negated as a result of increased energy levels within both the dielectric membrane and the cell gas.

The effects of a continuous potential across the compound during temperature-vacuum cycling would be significant only if the pressure (or temperature) change within the compound were sufficient to result in a discharge condition. If the conditions for discharge existed, the compound could be destroyed or grossly altered by the discharge phenomena.

b. Experimental

Two experiments are described to determine the effects of a vacuum environment on the discharge and breakdown potentials of cellular compounds.

The specimen configuration for both experiments was a four-inch cube containing an embedded point-place electrode pair as shown in Figure 3. The electrode spacing was 250 mils. The compounds used in these experiments were the CPR 23 Series and the Stafoam AA 600 Series at densities of 4, 8 and 20 lbs/ft^3.

All specimens were proportioned and cured as described in Table IV.

The first experiment had as its objective an observation of the effects of an applied potential on the specimens during the evacuation cycle. For this test six specimens, the three densities of both compounds, were used. The specimens, wired in parallel, were positioned in the vacuum chamber, and connected to the high voltage power supply and the detector network (Figure 4). A nichrome heating element was positioned around the specimens and attached to a Variac control. A thermocouple was embedded approximately a quarter (1/4) of an inch deep into an 8 lb/ft^3 specimen to obtain temperature data. The vacuum chamber was closed and the heater turned on. When the specimen temperature reached 100°C, a potential of 1 KVDC was applied to the plane electrodes. With the potential applied, vacuum pump-down was begun. During the voltage application period and the pump-down cycle, the corona detector was monitored for possible discharges within the specimens. The specimens were maintained at 100°C and 1×10^{-5} mm Hg for 48 hours with the 1 KVDC applied to the plane electrode. Throughout this time the corona detector was periodically monitored for evidence of discharges.

The second experiment had as its objective a determination of the effects of a continuously applied potential under conditions of high vacuum and high temperature on the discharge and breakdown potential of the test foams. For this experiment ten (10) specimens of each density for both the CPR 23 Series and the AA 600 Series materials were prepared, making a total of sixty specimens. These specimens were positioned in a test fixture, as shown in Figure 11. Each vertical row of specimens contained one specimen of each material at each of the three densities. The fixture containing the specimens was positioned in an aluminum bell jar (30 inches diameter x 36 inches high). Mounted to the exterior surface of the bell jar were Variac controlled heating elements capable of producing 6 kilowatts. The specimen temperatures were monitored using thermocouples which had been bonded to the specimen surface.

The specimens were connected to the high voltage power supply through leads attached to the common buss which provided support for each row of specimens by inserting the point electrode, with the plane electrode being terminated at ground. After the test set-up was completed, the vacuum and temperature conditioning was begun. The general conditions that were maintained during the test were a temperature of 100°C and a pressure of 10^{-5} mm Hg or less. The time to achieve these test conditions initially was 100 hours.

After achieving test conditions, corona discharge tests were made on one set of specimens. To make these measurements the column was connected to the high voltage power supply while the plane electrode of the specimen being tested was connected to the corona discharge detector. The plate electrodes for the five (5) remaining specimens were biased to the high voltage source to prevent their being stressed during the test. The voltage was then applied and increased at approximately 50 volts per second until a discharge (or breakdown) was observed. This procedure was repeated for each specimen on the column.

Upon completion of the corona discharge test, a potential of 10 KVDC was applied to each of the ten columns, with the plate electrode of each specimen at ground. This 10 KVDC potential was maintained throughout the 3000 hour test, with the exception of the corona discharge test intervals. Each corona discharge test required 5 to 8 hours. Periodically the discharge test was performed on the specimens of the initial column, and at each test interval an additional column was added to the discharge test until completion of the test period.

At the end of the 3000 hour period, all of the specimens were removed from the chamber and a final discharge and breakdown test was performed. This test was conducted at room-temperature and atmospheric pressure using the apparatus and method described in Paragraph IV, A, 3b. The purpose of this test was to determine the effects on the discharge and breakdown potentials of the continuous 10 KVDC stress combined with the intervals of higher potential produced during the corona discharge tests.

c. Results

The effects of a 1 KVDC applied potential on the specimens during the evacuation cycle were undetectable. Table X summarizes the occurrences of the experiment. It is noted that as a result of arcing from the high voltage leads within the chamber during the pump-down cycle, the applied potential was reduced from 1 KVDC to a minimum of 0.45 KVDC at a pressure of 5×10^{-4} mm Hg. The potential was increased to the 1 KVDC level when the pressure reached 1×10^{-4} mm Hg; this was maintained through the remainder of the test period. Previous attempts had been made to eliminate the arcing by insulating the high voltage leads with a heavy coating of silicone resin, but this method was not completely successful. Reducing the potential when an arc was observed in the chamber was done in an attempt to prevent overloading of the current-limited power supply and to monitor discharges within the specimens, since the arcing phenomenon was also recorded by the corona detector.

The only discharges monitored by the corona detector were coincidental with a visible arc from the high voltage leads within the chamber. After reaching a pressure of 1×10^{-4} mm Hg, at which time the potential was increased to the 1 KVDC level, no further discharges (or arcs) were observed on the detector through the duration of the test.

Upon completion of the forty-eight hour test, the specimens were removed from the chamber and dissected. No evidence of any discharge degradation could be observed within any of the specimens.

A summary of the results from the 10 KVDC continuous experiment follows. Based on the observable data, a maximum of four specimens failed as a result of the 10 KVDC applied potential; these were AA 620 - No. 6, AA 608 - Nos. 2 and 9, and CPR 23-4, No. 2. The remaining fifty-six specimens failed when the stress was greater than 10 KVDC either during discharge testing in the test environment or in the final discharge and breakdown evaluation after completion of the 3000 hour period.

During the initial discharge test after the specimens had reached temperature and pressure, it was observed that the discharge potential was approximately the same for each specimen and that the conductance levels were orders of magnitude greater than observed during the Preliminary Electrical Tests. Additional testing revealed that similar discharge potentials could be obtained by powering an electrode of one specimen and attaching the detector to a different specimen. This fact, combined with the high conductance levels, lead to the conclusion that the discharge being measured was a gaseous discharge in the chamber and not a specimen phenomenon. In an effort to obtain discharge data on the specimens, the system was returned to atmospheric pressure while maintaining the 93-100°C temperature. High voltage evaluations under these conditions again produced a gaseous conduction and not discharges within the specimens. The fact that no discharges were detected in the compounds for either condition may be due to 1) the close proximity of high and low potential sites within the system resulting in stresses causing gas conduction at potentials lower than those required to produce discharges within the compounds, or 2) the increased gas pressure within the cell as a result of elevated temperature creating discharge potentials within the compounds greater than those required to affect a discharge in the chamber environment.

At subsequent corona discharge test intervals, gas conduction again was the dominating phenomenon. Because of this, the discharge potential could be stated only as a "greater than" value; i.e., the discharge potential for the compound is greater than the gas conduction potential of the environment. Such a method does not specify the value of the discharge potential for the compound until it becomes less than the gas conduction potential for the environment. However, a "greater than" value is of engineering significance.

It may be noted from Table XI that only five of the original ten specimens for each compound was powered at 10 KVDC throughout the entire 3000 hours of the test. The other five specimens of each compound were powered at 10 KVDC for the periods of time indicated. The inability to supply an electrical load to these specimens is not explained, but is due to a cause external to the specimens since sets of specimens which were wired in common were neither powerable as sets nor individually. It is assumed that the cause of this problem is related to some type of surface leakage or gas conduction specific to the sets of specimens involved since all of these sets recovered prior to termination of the test. A comparison of the discharge and breakdown potentials for those specimens powered throughout the test with those powered for less than the entire test period shows there to be no significant difference. That is, the applied potential did not change the discharge or breakdown potential by an appreciable (if detectable) quantity. For example, the average breakdown potential for the CPR 23-8 powered specimens was 41 KVDC, while that of the unpowered was 40 KVDC.

At the completion of the 3000 hour environmental exposure, the applied potential was increased above the gas conduction potential to obtain breakdown data on each of the specimens without benefit of compound discharge information. Based on a subsequent discharge test at atmospheric pressure, it was determined that this evaluation produced breakdown in twenty-eight specimens.

The discharge analysis at atmospheric pressure and room-temperature showed the discharge potentials to be generally in the 20 to 40 KVDC range for those specimens which had not failed previously. No clear relationship between compound density and discharge potential was derived from these results.

The breakdown potential observations for both vacuum and atmospheric pressure indicate this potential to be a function of the compound density. This relationship between compound density and breakdown potential was observed in the Dielectric Characteristics Test, paragraph IV, A, 3.

Table XI and Figure 10 summarize the results of this continuous voltage application experiment.

3. Vibration Test

a. Discussion

To determine the characteristics of the foam materials under dynamic loading, a one-inch diameter brass sphere was embedded in the foam specimens and the specimens were subjected to various vibration loads. To the embedded sphere was mounted an accelerometer so that the natural frequency and transmissibility of the materials could be determined. Each specimen was first subjected to a 2g load and swept through a frequency range from 5 to approximately 2000 cps to determine the resonant or natural frequency associated with each specimen. After the resonance point was determined, the specimen was allowed to dwell at that frequency at 20g, 40g, and 60g to determine the characteristics of the specimens.

b. Experimental

The test specimens consisted of a five-inch cube of the test material foamed by pouring-in-place in an aluminum box. A brass sphere one inch in diameter was located in the approximate geometric center of each specimen. (The sphere was machined from material procured to Federal Specification QQ-B-626, Composition 22). A monitor accelerometer (Endevco, Model No. 2226) was bonded in a small cavity in the brass sphere. The accelerometer cable was brought out through the top of the specimen. The foam material was proportioned and mixed in accordance with the manufacturer's recommended instructions and cured as specified in Table IV. The box was etched using the standard sulfuric acid-sodium dichromate etchant prior to specimen preparation, resulting in good adhesion of the foam to the aluminum container. The top of the foam specimen was unsupported. Figure 12 is a photograph of the specimen configuration.

Each specimen, in turn, was mounted to a vibration exciter and subjected to sinusoidal vibration of 2.0g peak swept through the frequency range of 5 to 2000 cps to determine the specimen's natural or resonant frequency. After this natural frequency was determined, sinusoidal vibration dwell at 20g, 40g and 60g for 15 minutes at each level was performed. For specimens with a natural frequency greater than 2000 cps, the dwell was conducted at 200 cps. Time to failure of the specimens was noted. The failure criterion for breakdown of the foam was a discernible frequency shift associated with the sample under test. Specimens were dissected following test to verify the failure.

c. Results

The results of the vibration test are summarized in Table XII and Figures 13 and 14.

Although none of the specimens failed during the 2g sweep while determining the resonant frequency, both of the 4 lb/ft^3 density specimens failed at the start of the 20g dwell at resonant frequency. Furthermore, both of the 8 lbs/ft^3 density specimens failed during the 20g dwell, the CPR23-8 failing after 8.5 minutes at dwell while the Stafoam 608 failed after only 15 seconds at dwell. Since the resonant frequency of the 20 lbs/ft^3 density specimens was greater than 2000 cps, these specimens were vibrated at 200 cps. Both of these specimens survived 15 minutes at each of the three test levels (20, 4 and 60g's).

In analyzing the results, the area of compression was calculated by using the projected area of the brass sphere, $\pi(\frac{D}{2})^2$, where D is the diameter of the sphere. Using this expression, the area equals 0.785 in^2. The weight of the embedded sphere including the accelerometer was determined directly by weighing, and found to be 60 grams. (The density of the composite test sphere is 0.25 lbs/ft^3). Therefore, the static compressive stress on the foam resulting from the test sphere is 0.167 psi. Using this value, the input acceleration, and the transmissibility to the sphere at the test frequency, the dynamic stress can be calculated. Table XII includes a summary of the dynamic stresses on the foam for the various conditions of test.

The analysis subsequent to the determination of the dynamic characteristics of the foams tends to confirm the experimental results. In each case where the yield stress was exceeded, failure occurred immediately when testing at resonance began, i.e., when the applied load first exceeded the yield strength, as was the case for the CPR 23-4, Stafoam 604, and Stafoam 608 specimens. In the case where the applied dynamic load was slightly less than the yield strength, the specimen (CPR 23-8) failed only after 8.5 minutes. The analysis, of course, used calculations based on an average applied stress; therefore, these values would be expected to be lower than the actual maximum applied stress by some amount and would account for this failure (CPR 23-8) even though the yield was shown by analysis not to be exceeded. The two 20 lbs/ft^3 specimens, CPR 23-20 and Stafoam 620, were tested for 15 minutes at each of three test levels (20g, 40g and 60g) at a non-resonance point (200 cps as specified by the Contract) and exhibited no degradation. Stress associated with response at 200 cps is considerably below yield strength of the materials.

The transmissibility value for the CPR 23-8 appears somewhat low, based on both analysis and experimental results (see Figure 13). No explanation is postulated.

After vibration testing the specimens were dissected to determine the actual mode of failure. The four failed specimens, CPR 23-4, CPR 23-8, Stafoam 604 and Stafoam 608, all failed in an identical manner. The foam failure occurred in the immediate vicinity of the test sphere, leaving the sphere free to move in the specimen. Good adhesion of the foam to the sphere was evidenced by the fact that a thin film of foam (approximately .010 to .015 inch thick) still remained attached to the sphere.

The general conclusions based on these results and analysis are that the transmissibility and natural (resonance) frequency of the foams tested increases with increasing foam density, and the behavior of these materials under dynamic loads can be predicted reasonably well based upon analysis to determine their failure points.

4. Compressive Strength Test

a. Discussion

To determine the compressive properties of the six test materials, the Ultimate Compressive Strength, the Compressive Yield Strength at 0.2% Offset, and the Modulus of Elasticity were determined.

b. Experimental

The compressive properties of the foam materials were determined by testing in accordance with ASTM D695 (Method of Test for Compressive Properties of Rigid Plastics). The specimens were machined from pre-foamed blocks of the test materials. The pre-foamed blocks were prepared by mixing the ingredients in accordance with the manufacturer's instructions and pouring measured amounts of material into closed cavity molds, which had been preheated to 40-45°C. The specimens were cured at 100°C for 12 hours. The specimens used for these compressive property determinations were 2.00 x 2.00 x 2.00 inches.

c. Results

The results of the compressive property tests are presented in Table XIII.

5. Vacuum Weight Loss Test

a. Discussion

The weight loss of a plastic in a vacuum provides some indication of the material's usefulness in a low pressure environment. The weight loss and weight loss rate of materials in vacuum is dependent upon the quantity of low molecular weight fragments of the polymer, the formulation additives (including solvents, diluents, plasticizers, flame retardants, flexibilizers, etc.), the accelerator or catalyst used, and the adsorbed and absorbed materials (such as moisture, gases, mold releases, etc). The degree of cure, the amount of and nature of any by-products of the polymerization or curing process, and the temperature and pressure are also factors influencing the weight loss of the plastic material. (It should be noted that the pressure at which the test is conducted ceases to be a significant factor once the pressure reaches a value at which the mean free path of the gas molecules is equal to or greater than the test chamber dimensions).

In cellular plastics (foams), an important additional factor that will contribute to the "outgassing" of the material is the loss of the gas within the cells of the foam. The rate of loss of this gas is dependent upon not only the experimental design (specimen geometry, temperature and pressure of test, etc), but upon an important physical relationship between the specific gas and plastic material under consideration, known as the permeability constant (see Paragraph IV, B, 1).

The significance of the weight loss characteristics of a plastic in vacuum is that once known, they may be used to deduce certain information relating to the materials usefulness in a low pressure (vacuum) environment. Although the gross weight loss of a material in vacuum is helpful in characterizing the material, of greater signficance is the plot of weight loss rate as a function of time. These latter data define <u>when</u> the volatile products are given off. If the weight loss rate stabilizes at a low value (say 10^{-7} g/cm$^2\cdot$hr or lower) within the first day or two of testing, changes in engineering properties of the material as a result of the loss of these volatiles may be expected to occur extremely slowly, if at all. This conclusion remains valid whether the total weight loss is low or high, for if it is high, the major weight loss occurred in the early stages of the test.

On the other hand, if the weight loss rate is found to remain relatively high, more significant changes in engineering properties of the material may be expected to occur throughout the total time that the material is subjected to the vacuum environment. Furthermore, determination of the changes in specific properties of interest become proportionally more costly because of the increased testing time required, especially when considering applications in spacecraft requiring several years life now commonly specified.

In addition to changes in the properties of the materials, the outgassed products may produce a significant effect on other equipment aboard the spacecraft. Condensation of the products on electrical contacts, optical surfaces, or thermal control surfaces may render the affected part partially or totally inoperative. Contamination of the environment in the vicinity of an experiment on board a spacecraft may render the results of the experiment useless or, worse yet, lead to erroneous conclusions.

b. Experimental

Figure 15 is a photograph of the equipment used. A diagram of the experimental set-up is shown in Figure 16.

The vacuum system consisted of an oil diffusion pump with a liquid nitrogen cold trap and a vibration isolated mechanical pump. With use of the cold trap, pressures in the 10^{-7} mm Hg range are reached within the first hour in the set-up used for this test. The heater used to maintain the specimen at 80°C consisted of a glass cylinder wound with Nichrome wire, the input voltage of which was controlled by a Variac located outside the vacuum chamber. The temperature of the test specimen was monitored by a thermocouple embedded in a specimen identical to the test specimen, which was placed directly beneath it in the chamber. The balance used to monitor the weight of the specimen was a Cahn Gram Electrobalance, Model 1501, modified to allow the control and readout mechanisms to remain outside the vacuum chamber during the test.

The specimens were cut from pre-foamed blocks of the foam materials. The pre-foamed blocks were prepared by mixing the ingredients in accordance with the manufacturer's instructions and pouring measured amounts of material into closed cavity molds which had been preheated to 40-45°C. The material was cured as specified in Table IV. The specimens were approximately 1.2 x 1.2 x 0.12 inches.

The balance was zeroed and calibrated prior to commencement of each weight loss determination. The test specimen was placed on the balance arm sling and positioned within the heater. The temperature monitoring thermocouple embedded in a duplicate test specimen was located directly beneath the test specimen. The bell jar was lowered into position on the base plate and the initial specimen weight determined. Pump-down of the vacuum chamber was then initiated. After attaining an absolute pressure of 1 micron or less, the heater was turned on. Temperature stabilization at 80°C was achieved approximately 15 minutes after heater turn-on. Specimen weight and temperature, and chamber pressure were recorded periodically during the test. Final specimen weight was determined at atmospheric pressure and room temperature at the conclusion of the test.

c. Results

The total weight loss and the weight loss rate of the materials tested are presented in Figure 17. The Stafoam material is considerably better than the CPR material in total weight loss at the four pound per cubic foot density, exhibiting a loss of only 2% as compared to 4-1/4% for the CPR. At the eight pound per cubic foot density, both manufacturers' materials exhibited a weight loss of 1.9%. At the twenty pound per cubic foot density, the Stafoam material again exhibited a lower total loss, 1% as compared to 1.7% for the CPR material.

Comparing the weight loss rates of the various materials and densities, there is no significant difference between any of the test specimens, with the exception of the CPR 23-20. No measurable weight loss of the CPR 23-20 was noted after 75 hours in the test environment, which corresponds to a weight loss rate of 2×10^{-9} g/cm^2 hr or less.

6. Ultraviolet Radiation Stability

a. Discussion

To be suitable for use as encapsulants for high voltage equipment in a space environment, the electrical properties of the foam must not be adversely affected by this environment. Ultraviolet radiation is one component of this environment. To determine the effect of this ultraviolet radiation on the properties of the materials tested, specimens were subjected to energy in the range of .25 to .4 microns approximating solar intensity at 1 astronomical unit for 3000 hours at a pressure of 10^{-7} mm Hg.

From the xenon arc lamp used in this test as the source of ultraviolet radiation, infrared energy also was radiated. As a result, degradation of the foam could occur by at least two possible mechanisms; chemical degradation resulting directly from absorption of the ultraviolet energy by the polymer molecule (and/or other chemicals in the foam formulation) and thermal degradation resulting from absorption of the infrared energy from the radiation source. To minimize adverse thermal effects temperature control of the specimens was affected by an external fluid circulation system.

b. Experimental

A photograph of the experimental apparatus is shown in Figure 18. The apparatus consists of a vacuum chamber in the center of which is mounted the ultraviolet radiation source. Eight separate sample holders are spaced about the radiation source, each sample holder accommodating one foam specimen. The distance between the specimen and the source is fixed. The temperature of the sample holders was controlled by an external fluid circulation system; for this test the temperature of the specimens was maintained at approximately 100°C.

The ultraviolet radiation source was a Hanovia 2.2 kw xenon arc lamp. The ultraviolet output of the lamp, relative to its total output, changes in a slow and predictable manner as a function of time. This is compensated for during the duration of the 3000 hours exposure by increasing the power input to the lamp. The spectrum of the xenon lamp beyond 0.55 microns is shown in Figure 19. The radiation flux impinging on the specimen during this test was .07 to .09 watts/in^2 in the range of .25 to .4 microns, approximately the intensity of the sun at a distance of 1 astronomical unit.

The foam specimens used in this test were disks, approximately 2 inches in diameter and one-quarter inch thick.

The specimens were exposed to the ultraviolet radiation while in vacuum (10^{-7} mm Hg) at 100°C for 3048 hours. Periodically throughout the exposure, the specimens were removed from the apparatus, cooled to room temperature, and the following properties determined: dielectric constant, dissipation factor, physical dimensions, weight and visual appearance. While out of the exposure chamber the specimens were kept in a dessicator, except when being tested. The weight of the specimens was determined on a Mettler B-6 analytical balance and the dielectric constant and dissipation factor were determined in accordance with ASTM D 150, using a General Radio Micrometer-Electrode Specimen Holder.

c. Results

The results of the ultraviolet radiation stability test are presented in Table XIV. Examination of the data reveals that changes in the measured properties were insignificant. The surface of the specimen exposed to the ultraviolet energy darkened gradually from a white or off-white color to a dark brown in the first 1350 hours of exposure, after which no further darkening could be observed. All of the specimens reacted identically. Cross-sectioning the specimens revealed that the discoloration extended to a depth of less than 0.002 inch. Since most materials are opaque to ultraviolet radiation, the results of this test are as anticipated and suggest that any ultraviolet-sensitive components or devices should be embedded in the foam by at least 0.002 inch to provide shielding by the foam.

The temperature of the foam surface exposed to the ultraviolet radiation was maintained at 80°C during the early portion of the exposure. As the color of the surface darkened, the surface temperature increased until it stabilized at 100°C after approximately 1300 hours. For the remainder of the 3048 hour exposure, the surface temperature was maintained at approximately 100°C.

7. Thermal Impedance Test

a. Discussion

The purpose of the thermal impedance test was to determine by empirical means the equilibrium temperature of a foam specimen when a known amount of thermal energy is being dissipated within the specimen. For this test, a resistor embedded in the foam was the power dissipating component. The thermal energy developed by the resistor was dissipated through the component body and embedding foam, as well as the component leads. Because the relative quantities of heat dissipated through these two elements were not determined, and because of the inability to control adequately the many test variables (including component and test lead length conductor size, and thermal radiation properties of these test elements), no attempt was made to use the results of this test to calculate the thermal conductivity of the foam materials.

However, the results of this test are useful for approximating the temperature that might be expected from the dissipation of power within the foam material. In this test, various resistors were embedded in four-inch cubes of the foam materials and varying amount of power were dissipated by the resistors. The temperature of the resistor bodies and various locations within the foam cubes were monitored so that the thermal gradient at equilibrium could be determined.

Dissection of the foam specimen following the testing was performed to determine the nature and extent of any degradation resulting from the temperatures encountered.

b. Experimental

The specimen configuration is shown in Figures 20 and 21. The specimens were 4 x 4 x 4 inch cubes, with a resistor embedded in the approximate center of the specimen. The foam materials were proportioned and mixed in accordance with the manufacturer's instructions, poured into mold-released closed molds which had been pre-heated to 40-45°C, and then cured at 100°C for 24 hours. Thermocouples were embedded in the specimen (Figure 20) at the time of foaming.

Twenty-four specimens were prepared: four specimens for each manufacturer's material (CPR 23 Series and Stafoam 600 Series) at the three densities of interest (4, 8, and 20 lbs/ft^3). One resistor was embedded in each specimen. The resistors used were 1000 ohm, 5% resistors rated at 1-, 2-, 5-, and 10-watts. The 1- and 2-watt resistors were carbon composition while the 5- and 10-watt components were wire wound, procured to the following military specifications:

1-watt: MIL-R-11, Type RC32
2-watt: MIL-R-11, Type RC34
5-watt: MIL-R-26, Type RW57
10-watt: MIL-R-26, Type RW58

Six specimens were mounted in the test chamber at a time. Power and thermocouple leads were attached through feed-throughs to the chamber and a vacuum of 10^{-5} mm Hg was attained before power was applied to the embedded resistor. The resistors were first powered at room ambient temperature (22°C) at 10% of their rating. The temperature of the thermocouples embedded in the specimen were recorded until an equilibrium condition was achieved. The equilibrium condition is defined as that point at which the temperature rise of the resistor body is less than 0.5°C per hour. This generally required approximately 10 to 15 hours.

Following the room temperature 10% power test, the power input to the resistors was increased to 25% of their rated power and the test repeated. Following the room temperature testing, the vacuum chamber was heated to an ambient temperature of 80°C and the previously described tests repeated. The 80°C temperature was achieved by wrapping the vacuum chamber with tape heaters. The pressure of the vacuum chamber was returned to atmospheric pressure to reduce the heat-up time. After the ambient temperature was stabilized at 80°C, the chamber was evacuated and the testing at 10% and 25% of the resistor rating was performed.

Periodically throughout the test, the power input to the resistors, the temperature of the resistor body and the ambient temperature was recorded. After the equilibrium temperature condition was attained, the temperature of each of the four thermocouples in each specimen was recorded.

After testing, the specimens were dissected and visually examined for damage.

c. Results

The results of the thermal impedance test are presented in Table XV and Figure 22.

After testing, the specimens were dissected to determine the condition of the foam in the vicinity of the resistor.

All twelve of the one- and two-watt resistor specimens showed no evidence of any degradation as a result of the testing.

All six of the five-watt resistor specimens exhibited varying degrees of degradation.

(1) Both of the 20-lb density specimens (CPR 23-20 and Stafoam 620) discolored slightly to a light amber color for about 1/16 inch around the resistor. No other degradation was noted.

(2) The CPR 23-4 specimen was discolored light brown for about 1/8 inch around the resistor. No other degradation was noted.

(3) The remaining three specimens (CPR 23-8, Stafoam 604, and Stafoam 608) were discolored a dark brown for about 1/4 inch around the resistor and the foam originally in contact with the resistor was withdrawn approximately 1/8 inch (see Figure 23).

All six of the ten-watt resistor specimens also exhibited varying degrees of degradation.

(1) The least apparent damage occurred to the Stafoam 604 specimens. Within one-half inch of the resistors, the foam was discolored yellow (light brown). One of the specimen's exterior surfaces parallel to the axis of the resistor was bulged outward approximately 1/8 inch.

(2) The Stafoam 608 and 620, and the CPR 23-4 and 23-8 specimens were discolored for approximately 1/2 inch from the resistor. The color varied from dark brown to a yellow at about 1/2 inch. Each of the specimens except the Stafoam 608, had a charred void around the resistor for approximately 1/4 inch (Figure 24). The Stafoam 608 specimen did

not separate from the resistor body although some enlargement of foam cells near the resistor did occur. The Stafoam 608 and CPR 23-8 exhibited a bulge or swelling of approximately 1/16 inch on one exterior surface parallel to the central axis of the resistor.

These results indicate that temperatures above 300°F will cause degradation of the foam, at least in the vicinity of the hot component.

REFERENCES

1. Dunaetz, R. A. and Bahun, C. J., Foam-in-Place Dielectric Materials for Embedment of Aircraft and Space Vehicle Electronic Networks Operating at 3000 Volts; paper presented at the Sixth Electrical Insulation Conference, New York, New York, 13-16 September 1965.

2. Cuddihy, E. F. and Moacanin, J., Outgassing Rates in Polymeric Foams, NASA JPL Technical Report No. 32-840, 15 December 1965.

3. Bunker, E. R., Voltage Breakdown Problems at Low Air Pressures Encountered in the Mariner IV Spacecraft, from Proceedings of the Workshop on Voltage Breakdown in Electronic Equipment at Low Air Pressure, JPL Technical Memorandum 33-280, 15 December 1966.

4. Johnson, F. S., The Solar Constant, J. Meterorology, December 1954.

VI. Tables

TABLE I

SUMMARY OF MANUFACTURER'S REPORTED DATA

COMPOUND DESIGNATION (See Table for Manufacturer Identification)	Density, lbs/ft^3	Blowing Agent	Dielectric Strength volts/mil	Maximum Service Temp. °C	Cure Temperature °C	Exothermic Temperature °C	Compressive Strength psi		Flexural Strength psi	Moisture Absorption %	Dielectric Constant	Dissipation Factor
							//	⊥				
CPR 13	4	CO_2	-	138	120	155-160	82	58	-	1.76	-	-
	8	CO_2	-	138	120	155-160	260	170	-	1.35	-	-
	20	CO_2	-	138	120	155-160	1080	920	-	0.55	-	-
CPR 15	6	CO_2	-	138	120	155-160	170	170	-	1.0	-	-
	8	CO_2	-	138	120	155-160	280	280	-	1.0	-	-
	20	CO_2	-	138	120	155-160	1300	1300	-	1.0	1.38	.0024
CPR 18	4	CO_2	-	153	120	155-160	96	70	170	1.65	1.80	.0005
	8	CO_2	-	153	120	155-160	270	240	374	1.48	1.11	.0008
	20	CO_2	-	153	120	155-160	1500	1400	1100	1.10	1.50	.0026
CPR 21	4	CO_2	-	175	175	>155	100	-	-	1.7	-	-
	8	CO_2	-	175	175	>155	300	-	-	1.7	-	-
	20	CO_2	-	175	175	>155	1460	-	-	1.4	-	-
CPR 23	4	CO_2	-	175	175	155-160	100	70	-	1.7	1.08	-
	8	CO_2	-	175	175	155-160	300	230	-	1.7	1.15	-
	20	CO_2	-	175	175	155-160	1460	1300	-	1.4	1.4	-
CPR 33	4	CO_2	-	175	175	155	74	48	105	1.15	1.10	.0020
	8	CO_2	-	175	175	155	270	185	265	1.15	1.20	.0032
	20	CO_2	-	175	175	155	1250	1100	900	1.15	1.50	.0095
CPR 200	4	Freon	-	120	r.t.	~ 145	130	90	-	1.10	-	-
	8	Freon	-	120	r.t.	~ 145	340	250	-	0.80	-	-
	16	Freon	-	120	r.t.	~ 145	920	720	-	0.62	-	-
CPR 301	4	Freon	-	82	r.t.	~ 145	96	60	-	1.45	-	-
	8	Freon	-	105	r.t.	~ 145	270	240	-	1.30	-	-
	20	Freon	-	138	r.t.	~ 145	1400	1400	-	1.15	-	-
CPR 302	4	Freon	-	82	r.t.	~ 145	90	66	-	1.78	-	-
	8	Freon	-	105	r.t.	~ 145	260	220	-	1.45	-	-
	20	Freon	-	138	r.t.	~ 145	1000	1000	-	1.2	-	-
CPR 700	4	CO_2	-	120	120	-	115	100	-	1.30	-	-
	8	CO_2	-	120	120	-	320	300	-	1.08	-	-
	20	CO_2	-	120	120	-	1600	1500	-	1.10	-	-
CPR 727	4	CO_2	-	175	175	~ 160	100	76	-	0.80	-	-
	8	CO_2	-	175	175	~ 160	310	280	-	0.58	-	-
	20	CO_2	-	175	175	~ 160	1350	1300	-	0.48	-	-

TABLE I

SUMMARY OF MANUFACTURER'S REPORTED DATA (CONT'D)

COMPOUND DESIGNATION (See Table for Manufacturer Identification)	Density, lbs/ft^3	Blowing Agent	Dielectric Strength volts/mil	Maximum Service Temp. °C	Cure Temperature °C	Exothermic Temperature °C	Compressive Strength psi		Flexural Strength psi	Moisture Absorption %	Dielectric Constant	Dissipation Factor
							//	⊥				
STAFOAM 100	4	CO_2	-	150	107	-	120	-	-	2.93	1.08	.0005
	8	CO_2	-	150	107	-	220	-	-	1.10	1.17	.0005
	20	CO_2	-	150	107	-	920	-	-	0.21	1.38	.0024
STAFOAM 300	4	CO_2	-	82	r.t.	-	110	87	512	0.95	-	-
	8	CO_2	75	82	r.t.	-	320	283	-	0.70	-	-
	16	CO_2	-	82	r.t.	-	900	885	-	0.35	-	-
STAFOAM 400	4	CO_2	-	182	182	-	85	90	150	2.0	1.09	.00005
	8	CO_2	50	182	182	-	280	285	360	1.0	1.17	.00005
	20	CO_2	-	182	182	-	1340	1250	1650	0.28	1.40	.0028
STAFOAM AA 400	4	Freon	-	85	r.t.	-	90	51	-	25.0	1.08	-
STAFOAM AA 500	4	CO_2	-	165	120	-	85	75	145	1.75	-	-
	8	CO_2	-	165	120	-	272	272	312	1.57	-	-
	14	CO_2	-	165	120	-	585	585	565	1.46	-	-
STAFOAM AA 600	4	CO_2	-	165	120	-	98	72	172	1.95	-	-
	8	CO_2	-	165	120	-	245	225	380	1.92	-	-
	20	CO_2	-	165	120	-	1340	1340	1040	1.9	-	-
STAFOAM AA 1700	2	Freon	-	120	-	-	25	-	-	1.4	1.03	.001
	6	Freon	-	120	-	-	125	-	-	0.9	1.11	.002
	15	Freon	-	120	-	-	490	-	-	0.7	1.31	.004
POLYCEL 1100	2	Freon	-	94	-	-	26 at 10%		-	1.51	-	-
POLYCEL 1200	2	CO_2 Freon	-	175	-	-	34 at 10%		-	1.82	-	-
POLYCEL 1500	2	Freon	-	75	r.t.	-	25 at 10%		-	2.8	-	-
POLYCEL 1700	2	Freon	-	85	r.t.	-	22 at 10%		-	2.8	-	-
RN 9	2	Genetron	-	120	-	-	46 at 10%		-	1.8	-	-
RN 11	2	Genetron	-	120	-	-	29 at 10%		-	1.4	-	-
RN 18	2	Genetron	-	94	-	-	21 at 10%		-	-	-	-
MARAFOAM No. 3000	2	-	40	120	65	-	36		-	-	1.3	-
	6	-	42	120	65	-	150		-	-	1.4	-
	8	-	45	120	65	-	320		-	-	1.5	-

TABLE I

SUMMARY OF MANUFACTURER'S REPORTED DATA (CONT'D)

COMPOUND DESIGNATION (See Table for Manufacturer Identification)	Density, lbs/ft^3	Blowing Agent	Dielectric Strength volts/mil	Maximum Service Temp. °C	Cure Temperature °C	Exothermic Temperature °C	Compressive Strength psi		Flexural Strength psi	Moisture Absorption %	Dielectric Constant	Dissipation Factor
							//	⊥				
APCOFOAM No. 1414	4	Freon	-	-	-	-	120		-	3.0	-	-
	8	CO_2	-	-	-	-	300		-	1.2	-	-
	20	CO_2	-	-	-	-	1800		-	1.4	-	-
APCOFOAM No. 1419P	4	CO_2	110	-	-	-	100		-	3.3	1.2	.0005
	8	CO_2	120	-	-	-	320		-	3.0	1.3	.0007
	20	CO_2	200	-	-	-	1500		-	3.0	1.4	.001
SILASTIC S-5370	10	-	-	205	-	-	60		-	-	1.17	.001
R-7002	14	N2/H2	-	345	165	-	220 (10%)		-	5.0	1.25	-
R-7003	16	-	-	345	165	-	325 (10%)		-	5.0	1.26	-
Epi-Rez Epi-Cure	2	Freon	-	-	r.t.	-	16	18	-	1.8	-	-
DYLITE	2	-	50	80	-	-	30 (5%)		90	1.1	1.02	.0005
	4	-	-	80	-	-	70 (5%)		200	0.7	-	-
	20	-	-	80	-	-	-		-	-	-	-
URALANE 573	2	Freon	-	120	23	-	25		-	2.0	-	-
	10	Freon	-	-	23	-	290		-	2.0	-	-
URALANE 574	2	Freon	-	120	23	-	24		-	2.0	-	-
	6	Freon	-	-	23	-	110		-	2.0	-	-
RTV 757	44	-	-	310	120	-	-		-	-	-	-
RTV 7	12-16	-	147	-	r.t.	-	0.5 (10%)		-	-	1.8	-
ABLEFOAM No. 1	10	NH_4CO_3	-	175	65	-	340		-	-	1.51	.0114
	15	NH_4CO_3	80	175	65	-	530		-	-	1.65	.0169
	20	NH_4CO_3	-	175	65	-	900		-	-	1.93	-
URALANE 1723	6	Freon	-	120	23	-	130 (5%)		-	3.0	-	-
XR-5017	20-25	-	80	260	r.t.	-	12.2(25%)		-	0.01	2.8	-
SCOTCHCAST No. 603	6	-	50	94	110	-	50		-	1.5	-	-
ECCOFOAM FP	2	CO_2	-	107	65	-	50		-	1.5	1.04	.0002
	6	CO_2	37	107	65	82	200		-	1.3	1.10	.0003
	18	CO_2	-	107	65	-	700		-	0.2	1.3	.001

TABLE I
SUMMARY OF MANUFACTURER'S REPORTED DATA (CONT'D)

COMPOUND DESIGNATION (See Table for Manufacturer Identification)	Density, lbs/ft^3	Blowing Agent	Dielectric Strength volts/mil	Maximum Service Temp. °C	Cure Temperature °C	Exothermic Temperature °C	Compressive Strength psi //	Compressive Strength psi ⊥	Flexural Strength, psi	Moisture Absorption, %	Dielectric Constant	Dissipation Factor
ECCOFOAM FPH	4	CO_2	-	205	150	-	120		-	1.0	1.06	.0001
	8	CO_2	-	205	150	-	300		-	0.2	1.12	.0003
	14	CO_2	-	205	150	-	600		-	0.1	1.25	.001
ECCOFOAM EFF	4	Celogen	-	175	120	-	100		-	1.0	1.08	.003
	10	Celogen	-	175	120	-	400		-	1.0	1.15	.006
	15	Celogen	-	175	120	-	700		-	1.0	1.3	.010
ECCOFOAM SIL	20	-	-	260	120	-	10 (25%)		-	-	1.3	.01
ECCOFOAM GH	20	-	-	175	120	10°above cure temp.	600		-	1.0	1.48	.009
NOPCOFOAM A 200	6	CO_2	-	120	94	165	150		-	-	1.12	-
	10	CO_2	48	120	94	165	400		-	0.9	1.08	.0004
	16	CO_2	-	120	94	165	800		-	0.8	1.31	.0017
NOPCOFOAM B 600	10	CO_2	-	162	150	175	290		-	-	1.09	.002
	14	CO_2	-	162	150	175	450		-	-	1.12	.003
NOPCOFOAM BH 600	10	CO_2	41	215	175	175	290		-	-	1.2	.003
NOPCOFOAM BX105	2.5	CO_2	-	120	-	165	37	23	45	-	-	-
	6	CO_2	-	120	-	165	160	150	150	-	-	-
	20	CO_2	-	120	-	165	910		-	-	-	-
NOPCOFOAM BX212	2.5	CO_2	-	120	94	165	50	21	78	-	1.05	-
	6	CO_2	-	120	94	165	190	145	240	-	1.10	-
	15	CO_2	-	120	94	165	700	720	780	-	1.18	-
NOPCOFOAM BX249	2	Freon	-	120	45	-	30	20	-	2.0	1.05	-
NOPCOFOAM BX251	2	Freon	-	175	65	-	45	30	-	2.0	1.05	-
NOPCOFOAM C-600	5	CO_2	-	120	94	165	120		-	1.5	1.1	.00002
	8	CO_2	-	120	94	165	260		-	3.5	1.1	.0007
	14	CO_2	-	120	94	165	800		-	3.0	1.15	.002
NOPCOFOAM CA-600	20	CO_2	-	74°	r.t.	150	920		-	3.0	-	-
NOPCOFOAM G-300	4	CO_2	-	150	135	160	85		-	2.0	1.10	-
	6	CO_2	-	150	135	160	160		-	1.0	1.12	-

TABLE I

SUMMARY OF MANUFACTURER'S REPORTED DATA (CONT'D)

COMPOUND DESIGNATION (See Table for Manufacturer Identification)	Density, lbs/ft^3	Blowing Agent	Dielectric Strength volts/mil	Maximum Service Temp. °C	Cure Temperature °C	Exothermic Temperature °C	Compressive Strength psi		Flexural Strength psi	Moisture Absorption %	Dielectric Constant	Dissipation Factor
							//	⊥				
NOPCOFOAM G-500	2	CO_2	-	82	r.t.	150	30	20	-	3.2	-	-
	4	CO_2	-	82	r.t.	150	75	55	-	2.3	-	-
	6	CO_2	-	82	r.t.	150	150	120	-	1.2	-	-
NOPCOFOAM P-500	2	CO_2	-	74	r.t.	6(10%)	-	-	-	6.7	2.2	-
	6	CO_2	47	74	r.t.	85(10%)	-	-	-	-	2.0	-
SCOTCHCAST XR 5068	15	-	40	-	120	-	570	-	-	-	2.0	0.03

TABLE II

COMPOUND AND MANUFACTURER'S IDENTIFICATION

Compound Designation	Manufacturer
CPR 13 15 18 21 23 33 200 301 302 700 727	CPR Division, The Upjohn Company Torrance, California
Stafoam 100 300 400 AA400 AA500 AA600 AA1700 Polycel 1100 1200 1500 1700	Polytron Company Richmond, California
RN 9 11 18	Allied Chemical, National Aniline Division New York, N. Y.
Marafoam 3000	Marblette
Apcofoam 1414 1419P	Allied Plastics Co., Inc. El Segundo, California
Silastic S 5370 R 7002 R 7003	Dow Corning Corporation Midland, Michigan
Epi-Rez 2252 Epi-Cure 876	Jones-Dabney Company Louisville, Ky.
Dylite	Sinclair-Koppers Company Pittsburgh, Penn.
Uralane 573 574 1723	Furane Plastics, Inc. Los Angeles, California
RTV 7 757	General Electric Co. Waterford, New York
Ablefoam 1	Ablestick Adhesive Co. Gardena, California
Scotchcast 603 XR-5017 XR-5068	Minnesota Mining and Mfg. Co. St. Paul, Minn.
Eccofoam FP FPH EFF SIL GH	Emerson and Cuming, Inc. Canton, Mass.
Nopcofoam A-200 B-600 BH-600 BX-105 BX-212 BX-249 BX-251 C-600 CA-600 G-300 G-500 P-500	Nopco Chemical Company Newark, New Jersey

TABLE III

CHARACTERISTICS OF MATERIALS FOR LABORATORY TESTING

The listed characteristics are property goals on which selection of materials for laboratory testing was based.

Closed cell structure formulation, with low outgassing rates.

Good mechanical and electrical characteristics at extremes of temperature.

Reasonable work life of the mixed compound.

Good mechanical and electrical properties at low foam densities.

Ease of handling and mixing of the compound.

Minimum storage requirements - good shelf life.

Exothermic temperature and heat cure limited to 150°C.

Stable dimensional and physical characteristics with prolonged vacuum exposure.

Stable dimensional and physical characteristics with thermal cycling and aging.

High dielectric strength.

TABLE IV

MATERIALS SELECTED FOR PRELIMINARY TEST

Compound Designation	Density (lbs/ft^3)	Mix Ratios (pbw)	Recommended Cure (°C/hours)	Cure Schedule used in this Program(°C/hrs)
CPR 23	4	R-36 T-64	178/2	100/12
	8	R-38.7 T-61.3	178/2	100/12
	20	R-41.2 T-58.8	178/2	100/12
*CPR 200	4	R-36.9 TA-63.1	71/.5	
	8	R-38 TA-62	71/.5	
	20	R-39.1 TA-60.9	71/.5	
CPR 727	4	R-30.5 T-69.5	178/2	100/12
	8	R-32.2 T-67.8	178/2	100/12
	20	R-36.0 T-64.0	178/2	100/12
Eccofoam EFF	4	NA	125/3	125/3
	10	NA	125/3	125/3
	15	NA	125/3	125/3
Eccofoam FPH	4	R-100 12-4H-75	150/3	100/12
	8	R-100 12-6H-75	150/3	100/12
	20	R-100 12-10H-85	150/3	100/12

Compound Designation	Density (lbs/ft^3)	Mix Ratios (pbw)	Recommended Cure (°C/hours)	Cure Schedule used in this Program(°C/hrs)
Nopcofoam BX-249	2	R-44 T-56	60/24	80/2
*Nopcofoam G-300	4	R-36 T-64	130/?	
	6	R-39 T-61	130/?	
*Stafoam 100	4	Comp 1-100 Comp 2-104	130/6	
	8	Comp 1-100 Comp 2-89.6	130/6	
	20	Comp 1-100 Comp 2-82.8	130/6	
Stafoam 600	4	Comp 1-100 Comp 2-147.7	130/6	100/10
	8	Comp 1-100 Comp 2-114.2	130/6	100/10
	20	Comp 1-100 Comp 2-98	130/6	100/10

* Material eliminated from preliminary testing when unable to obtain satisfactory specimens for test.

TABLE V

THERMAL CYCLING RESULTS

Page 1 of 3

Compound and Specimen Type	*Specimen Weight (grams)			Specimen Dimensions (inches)		
	Before	After	% Change	Before	After	% Change
Eccofoam FPH, 12-4H Billet	222.2	217.0	-2.2	9.992 5.005 4.000	9.992 5.010 4.006	.00 +.10 +.15
Eccofoam FPH, 12-6H Billet	473.1	467.5	-1.2	9.973 4.998 4.006	10.020 5.016 4.042	+.48 +.36 +.90
Eccofoam FPH, 12-10H Billet	1083.4	1079.7	-0.4	9.966 5.002 4.001	9.994 5.022 4.021	+.28 +.39 +.50
Eccofoam FPH, 12-4H Al Box	310.8	308.3	-0.8	10.448 4.122 5.023	10.444 4.114 5.022	-.40 +.50 .00
Eccofoam FPH, 12-6H Al Box	450.0	451.0	-1.6	10.486 4.046 5.108	10.482 4.073 5.110	-.40 +.67 +.40
Eccofoam FPH, 12-10H Al Box	1192.0	1187.5	+0.4	10.339 4.580 5.140	10.479 4.370 5.223	-.09 +.49 +.25
CPR 23-4 Billet	267.8	262.7	-1.9	9.983 4.995 3.994	9.966 4.992 3.986	-.17 -.06 -.20
CPR 23-8 Billet	495.4	489.0	-1.3	9.973 4.993 3.995	9.959 4.988 3.991	-.16 -.10 -.10
CPR 23-20 Billet	1169.7	1165.9	-0.3	9.962 4.982 3.988	9.952 4.979 3.990	-.10 -.06 -.10
CPR 23-4 Al Box	266.2	263.6	-1.0	10.470 4.026 5.008	10.459 4.018 5.014	-.11 -.19 +.12
CPR 23-8 Al Box	437.3	434.7	-0.6	10.463 4.046 5.041	10.448 4.048 5.044	+.34 -.05 +.06
CPR 23-20 Al Box	1068.5	1066.5	-0.2	10.453 4.040 5.062	10.459 4.039 5.065	.00 .00 +.06
CPR 727-8 Billet	419.8	413.0	-1.6	9.938 4.974 3.978	9.899 4.957 3.967	+.61 -.34 -.28
CPR 727-20 Billet	1133.6	1126.8	-0.6	9.915 4.966 3.976	9.908 4.965 3.972	-.07 .00 -.10

* Weight given is of foam only, excludes Al box and thermocouple when applicable.

TABLE V

THERMAL CYCLING RESULTS (cont'd)

Page 2 of 3

Compound and Specimen Type	*Specimen Weight (grams)			Specimen Dimensions (inches)		
	Before	After	% Change	Before	After	% Change
CPR	229.2	225.0	-1.8	10.453	10.457	+.03
727-4				4.032	4.052	-.50
Al Box				5.001	5.002	+.20
CPR	456.4	451.5	-1.1	10.449	10.445	-.03
727-8				4.044	4.029	-.40
Al Box				5.012	5.025	+.26
CPR	1099.4	1097.5	-0.1	10.443	10.440	-.02
727-20				4.015	4.020	+.07
Al Box				5.018	5.030	+.20
Nopcofoam	231.1	226.6	-1.9	9.980	9.953	-.28
G-302				4.993	4.982	-.18
Billet				3.996	3.985	-.28
Nopcofoam	454.5	448.7	-1.3	9.996	9.950	-.16
G-306				4.988	4.979	-.18
Billet				3.993	3.990	-.08
Nopcofoam	1217.2	1213.9	+0.3	9.971	9.961	-.10
G-320				4.996	4.988	-.16
Billet				4.008	4.005	-.07
Nopcofoam	225.8	222.0	-1.7	10.411	10.416	+.05
G-302				4.220	4.212	-.20
Al Box				5.044	5.044	.00
Nopcofoam	456.4	452.7	-0.8	10.452	10.437	-.01
G-306				4.104	4.102	.00
Al Box				5.093	5.076	+.03
Nopcofoam	1187.5	1188.0	-0.0	10.418	10.408	-.10
G-320				4.205	4.225	-.47
Al Box				4.970	5.011	+.82
Nopcofoam	157.7	146.4	-7.0	10.008	11.163	+11.5
BX249-N				5.008	5.856	+16.9
Billet				4.005	4.555	+13.7
Nopcofoam	496.3	464.4	-6.4	9.975	10.055	+.80
BX249-6				4.995	5.086	+.18
Billet				3.996	3.999	+.07
Nopcofoam	176.4	174.2	-1.3	10.428	10.356	-.69
BX249-N				4.203	4.540	+8.10
Al Box				5.110	5.755	+14.5
Nopcofoam	460.9	439.8	-4.4	10.447	10.442	-.04
BX249-6				4.130	4.161	+.75
Al Box				5.031	5.067	+.71
Stafoam	236.5	231.6	-2.1	9.958	9.924	-.34
AA604				4.984	4.973	-.22
Billet				3.975	3.969	-.15

* Weight given is of foam only, excludes Al box and thermocouple when applicable.

TABLE V

THERMAL CYCLING RESULTS (cont'd)

Compound and Specimen Type	*Specimen Weight (grams)			Specimen Dimensions (inches)		
	Before	After	% Change	Before	After	% Change
Stafoam AA608 Billet	383.6	378.3	-1.4	9.978 5.000 4.015	9.957 4.998 4.009	-.11 -.40 -.09
Stafoam AA620 Billet	1216.2	1213.9	-0.2	9.973 4.983 3.982	9.965 4.980 3.982	-.07 -.6 .00
Stafoam AA604 Al Box	220.7	221.1	+0.2	10.464 4.051 5.026	10.454 4.064 5.009	-.09 +.32 -.30
Stafoam AA608 Al Box	372.5	371.5	-0.3	10.486 4.083 5.089	10.481 4.094 5.090	-.05 +.27 +.02
Stafoam AA620 Al Box	1146.3	1146.5	-0.0	10.436 4.060 5.010	10.442 4.057 5.013	+.06 -.02 +.06

* Weight given is of foam only, excludes Al box and thermocouple when applicable.

TABLE VI

CORONA DISCHARGE AND BREAKDOWN TEST RESULTS FOR VARIOUS ELECTRODE SPACINGS AND COMPOUND DENSITIES

Specimen	Density (lbs/ft^3)	Gap (Mils)	* Polarity	Corona Potential (KVDC)	Corona Current (10^{-9} Amps)	Breakdown Potential (KVDC)	Dielectric Strength (Volts/Mil)
FPH 12-4H	4	50	Pt grd	13.5	>>20	13.5	270
FPH 12-4H	4	50	Pt grd	7.5	>>20	7.5	150
FPH 12-4H	4	50	Pt grd	10	20	16	200
FPH 12-4H	4	250	Pt grd	24	8	55	220
FPH 12-4H	4	250	Pt grd	30	> 20	40	160
FPH 12-4H	4	250	Pt grd	35	20	43	172
FPH 12-10H	22	50	Pt grd	29.5 35	4 8-10	56	1130
FPH 12-10H	22	50	Pt grd	-	-	64	1270
FPH 12-10H	22	50	Pl grd	-	-	68	1360
FPH 12-10H	22	50	Pt grd	-	-	47	940
FPH 12-10H	22	100	Pl grd	-	-	68	680
FPH 12-10H	22	113	Pl grd	-	-	64	566
FPH 12-10H	22	125	Pl grd	-	-	53	425
FPH 12-10H	22	125	Pt grd	34.5	8	70	560
FPH 12-10H	22	125	Pt grd	23 38	2 8	53	425
FPH 12-10H	22	132	Pl grd	-	-	60	455
FPH 12-10H	22	250	Pl grd	-	-	76	304
FPH 12-10H	22	250	Pt grd	20 30 40	15-20 40 100	54	226
FPH 12-10H	22	250	Pt grd	36 52	8 20	97	388
FPH 12-10H	22	250	Pt grd	30	8	66	264

* Pt grd = Point electrode is ground
Pl grd = Plate electrode is ground

TABLE VII

EFFECT OF SUSTAINED TIME AT CORONA POTENTIAL

Specimen	Density (lbs/ft^3)	Gap (Mils)	* Polarity	Corona Potential (KVDC)	Corona Current (10^{-9} Amps)	Breakdown Potential (KVDC)	Dielectric Strength Volts/Mil	Remarks
FPH 12-4H	4	1000	Pt grd	64	4-6			Failed after 30 mins. at 79.5 KVDC
				70	10-12			
				79.5	15-30	79.5		
FPH 12-10H	22	1000	Pt grd	60	4			After 15 minutes at 82 KVDC, test discontinued without specimen failure. Specimen was dissected and start of breakdown path was observed at point electrode.
				70	15			
				70	20-40			
				75	30			
				75	80-100			
				82	100			

* Pt grd = Point electrode is ground
Pl grd = Plate electrode is ground

TABLE VIII

COMPOUND CORONA DISCHARGE AND BREAKDOWN TEST RESULTS

Specimen	Density (lbs/ft^3)	Gap (Mils)	* Polarity	Corona Potential (KVDC)	Corona Current (10^{-9} Amps)	Breakdown Potential (KVDC)	Dielectric Strength (Volts/Mil)
CPR 23-4	4	125	Pt grd	26	>>20	26	208
CPR 23-8	8	125	Pt grd	28	> 8	45	360
CPR 23-20	20	125	Pt grd	38	> 8	48	394
CPR 727-4	4	125	Pt grd	27.5	>>20	27.5	220
CPR 727-8	8	125	Pt grd	17.5	> 8	17.5	140
CPR 727-20	20	125	Pt grd	30	>> 20	30	240
G-302	4	125	Pt grd	32.5	>> 20	32.5	260
G-306	8	125	Pt grd	34	~ 8	52	416
G-320	20	125	Pt grd	36	> 8	41	328
AA 604	4	125	Pt grd	25	> 8	25	200
AA 608	8	125	Pt grd	31.5	20	31.5	262
AA 620	20	125	Pt grd	27.5	20	40	320
BX 249-N	4	125	Pt grd	44	5	54	432
BX 249-6	8	125	Pt grd	48	4	64	512
FPH 12-4H	4	125	Pt grd	20	20	33	264
FPH 12-6H	8	125	Pt grd	35	>> 20	35	280
FPH 12-10H	20	125	Pt grd	32	~ 8	64	512

* Pt grd = Point electrode is ground

TABLE IX

GASEOUS PERMEABILITY RATE DATA

Time (hrs)	Stafoam AA 604 (mm Hg)	Stafoam AA 608 (mm Hg)	Stafoam AA 620 (mm Hg)	CPR 23-4 (mm Hg)	CPR 23-8 (mm Hg)	CPR 23-20 (mm Hg)	Room Temp./ Atm. Pressure ($^{\circ}$C/mm Hg)	Vacuum Pressure (mm Hg)
0	747	752	757	744	747	761	25/760	--
3	757	750	757	744	757	761	25/760	50x10^{-3}
23	739	746	757	739	759	765	25/760	25x10^{-3}
48	737	742	761	739	761	777	25/760	10x10^{-3}
73.5	733	740	765	739	761	781	25/760	10x10^{-3}
143.5	729	739	772	733	762	794	25/760	1.5x10^{-3}
215	723	726	777	728	763	806	25/760	1.5x10^{-3}
312	714	718	778	718	760	816	25/760	1.5x10^{-3}
408	701	706	776	707	750	819	23/763	1.5x10^{-3}
530	691	697	776	698	743	824	24/763	1.5x10^{-3}
674	684	692	778	694	741	835	25/763	1.5x10^{-3}
746	677	685	776	687	734	835	25/763	1.5x10^{-3}
818	670	679	771	683	730	835	25/762	$< 10^{-3}$
914	662	672	767	677	723	834	23/761	$< 10^{-3}$
986	658	669	765	673	719	834	23/759	$< 10^{-3}$
1082	648	661	760	666	713	832	23/763	$< 10^{-3}$
1154	644	656	754	663	708	829	23/763	$< 10^{-3}$
1250	640	653	754	661	705	830	23/763	$< 10^{-3}$
1322	636	649	751	658	702	829	23/763	$< 10^{-3}$
1494	632	647	749	657	699	829	24/765	$< 10^{-3}$
1542	628	643	748	655	697	828	24/763	$< 10^{-3}$
1614	622	637	743	649	691	824	23/767	$< 10^{-3}$
1662	618	633	740	647	687	822	23/767	$< 10^{-3}$
1758	613	629	736	644	683	819	23/765	$< 10^{-3}$
1830	612	627	736	643	684	819	24/767	$< 10^{-3}$
1966	598	616	726	635	672	812	23/765	$< 10^{-3}$
2206	588	605	717	628	663	803	24/767	$< 10^{-3}$
2360	580	599	712	623	656	797	24/767	$< 10^{-3}$
2514	574	593	706	618	650	791	24/767	$< 10^{-3}$
2710	566	586	700	614	646	785	24/760	$< 10^{-3}$
3238	548	569	684	601	630	767	24/769	$< 10^{-3}$
*Volume N_2 Gas in Test Apparatus(cc)	54.7	58.9	74.5	60.1	56.0	63.6		

* Volume at start of test.

TABLE X

CORONA EVALUATION DURING VACUUM CHAMBER PUMP-DOWN

TIME (Hours)	PRESSURE (mm Hg)	POTENTIAL (KVDC)	DISCHARGE CURRENT (10^{-9} Amps)	REMARKS
0	760.	1.00	-	no observable change
.1	10.	1.00	-	
.2	5.	1.00	gas conduction occurred in test chamber above listed potential	
.3	0.5	0.80		
.4	0.2	0.60		
.5	0.02	0.50		
1.0	0.0005	0.44		
1.5	0.0003	0.48		
1.8	0.0002	0.70		
2.0	0.00015	1.00	none detected	
6.0	0.00005	1.00		
20.0	0.00001	1.00		
24.0	0.00001	1.00		
48.0	0.00001	1.00		
after 48	760.	-	-	specimens dissected - no evidence of discharge in any specimen.

TEST TEMPERATURE: 100°C

TABLE XI (Sheet 1 of 6)

RESULTS OF CORONA DISCHARGE AND BREAKDOWN TESTS

Material	Time (Hours)	Specimen Number									
		1	2	3	4	5	6	7	8	9	10
CPR 23-4	100	22. (200) [22.] F/	↑								
	500	[4.] PF/		10. 1/							
	1500	[1.] PF/	2/	17. 1/	↑ 3/	↑ 3/	20. 1/			↑ 3/	↑ 3/
	2050		↓		↓	↓		21. 1/		↓	↓
	3000	[<1.] PF/	[<1.]	~20. [33.] 1/ F/	~20. [46.] 1/ F/	~20. [40.] 1/	~20. [39.] 1/ F/	~20. [31.] 1/ F/	~20. [44.] 1/	[3.]	[7.]
↓	3000 at 1 ATM	[2.] PF/	[3.]	[7.]	25. [25.] PF/	26. (2000) [36.] F/	[11.] PF/	[1.] PF/	37. [37.] F/	11. (750) [13.] F/	[8.]

Information Key:

Discharge Potential in KVDC

(Discharge Current) in 10^{-9} amps

[Breakdown Potential in KVDC]

Notes: 1/, 2/, 3/, etc.

Notes:
1/ gas conduction external to specimen.
2/ column not powerable from start to 3000 hours.
3/ column not powerable from 1500 to 3000 hours.
4/ arcing external to specimen
F/ specimen failed
PF/ specimen failed previously

TABLE XI (Sheet 2 of 6)

RESULTS OF CORONA DISCHARGE AND BREAKDOWN TESTS

Material	Time (Hours)	Specimen Number 1	2	3	4	5	6	7	8	9	10
CPR 23-8	100	25. 1/	↑								
│	500	30. 1/	│	24 1/							
│	1500	20. 1/	2/	17. 1/	↑ 3/	↑ 3/	20. 1/			↑ 3/	↑ 3/
│	2050		↓		↓	↓	20. 1/	20. 1/		↓	↓
│	3000	~20. [34.] 1/	~20. [35.] 1/ F/	~20. [33.] 1/	~20. [46.] 1/ F/	~20. [44.] F/	~20. [40.] F/	~20. [30.] 1/	~20. [35.] 1/	[3.] 1/	~20. [32.] 1/ F/
↓	3000 at 1 ATM	17. (>400) [30.] F/	[14.] PF/	39. (2000) [45.] F/	[3.5] PF/	20. (2000) [32.]	20. [20.] PF/	26. (300) [37.] F/	34. (2500) [54.] F/	30. (2500) [46.] F/	[2.) PF/

Information Key:

Discharge Potential
in KVDC
(Discharge Current)
in 10^{-9} amps

[Breakdown Potential]
in KVDC

Notes: 1/, 2/, 3/, etc.

Notes:

1/	gas conduction external to specimen
2/	column not powerable from start to 3000 hours
3/	column not powerable from 1500 to 3000 hours
4/	arcing external to specimen
F/	specimen failed
PF/	specimen failed previously

TABLE XI (Sheet 3 of 6)
RESULTS OF CORONA DISCHARGE AND BREAKDOWN TESTS

Material	Time (Hours)	Specimen Number									
		1	2	3	4	5	6	7	8	9	10
CPR 23-20	100	24. 1/	↑								
│	500	24. 1/	│	21. 1/							
│	1500	20. 1/	2/	17. 1/	↑ 3/	↑ 3/	20. 1/			↑ 3/	↑ 3/
│	2050		↓		↓	↓		18. 1/		↓	↓
│	3000	∼20. [44.] 1/	∼20. [35.] 1/	∼20. [30.] 1/	∼20. [45.] 1/	∼20. [37.] 1/	∼20. [50.] 1/	∼20. [31.] 1/	∼20. [42.] 1/	∼20. [42.] 1/	∼20. [41.] 1/
↓	3000 at 1 ATM	40. (150) [73.] F/	23. (>2000) [35.5] F/	44. (∼300) [56.] F/	42. (∼750) [60.] F/	46. (600) [64.] F/	54. (1000) [>82.] 4/	53. [53.] F/	41. [41.] F/	48. (1500) [53.] F/	50. (1500) [>80.] 4/

Information Key:

Discharge Potential
in KVDC

(Discharge Current)
in 10^{-9} amps

[Breakdown Potential]
in KVDC

Notes: 1/, 2/, 3/, etc.

Notes:
1/ gas conduction external to specimen
2/ column not powerable from start to 3000 hours
3/ column not powerable from 1500 to 3000 hours
4/ arcing external to specimen
F/ specimen failed
PF/ specimen failed previously

TABLE XI (Sheet 4 of 6)

RESULTS OF CORONA DISCHARGE AND BREAKDOWN TESTS

Material	Time (Hours)	Specimen Number									
		1	2	3	4	5	6	7	8	9	10
AA 604	100	21. 1/	2/								
	500	30. 1/		19. 1/							
	1500	30. 1/		19. 1/	3/	3/	17.5 [17.5] 1/ F/			3/	3/
	2050							25. 1/			
	3000	∼20. [35.] 1/ F/	∼ 20. [37.] 1/ F/	∼20. [28.] 1/ F/	∼ 20. [46.] 1/ F/	∼20. [45.] 1/ F/	[< 1.] PF/	∼20. [30.]	∼20. [41.] 1/ F/	8. 1/	∼ 20. [38.] 1/ F/
	3000 at 1 ATM	16. (250) [18.] PF/	[< 1.] PF/	[< 1.] PF/	[3.]	[8.]	[< 1.] PF/	20. (1500) [23.] F/	[< 1.] PF/	18. [18.] F/	23. [23.] PF/

Information Key:

Discharge Potential
in KVDC

(Discharge Current)
in 10^{-9} amps

[Breakdown Potential]
in KVDC

Notes: 1/, 2/, 3/, etc.

Notes:	
1/	gas conduction external to specimen
2/	column not powerable from start to 3000 hours
3/	column not powerable from 1500 to 3000 hours
4/	arcing external to specimen
F/	specimen failed
PF/	specimen failed previously

TABLE XI (Sheet 5 of 6)
RESULTS OF CORONA DISCHARGE AND BREAKDOWN TESTS

Material	Time (Hours)	Specimen Number 1	2	3	4	5	6	7	8	9	10
AA 608	100	25. 1/	↑								
	500	30. [30.] 1/F/	2/	24. 1/							
	1500	6. [6. 1/PF/		17. 1/	3/	3/	20. (~500) 1/			3/	3/
	2050		↓		↓	↓		24. 1/		↓	↓
	3000	[<1.] PF/	[4.]	~20. [28.] 1/ F/	~20. [46.] 1/ F/	~20. [44.] 1/ F/	~20. [37.] 1/ F/	~20. [28.] 1/ F/	~20. [20.] 1/	[7.5]	[3.]
↓	3000 @ 1 Atm	[1.] PF/	[9.]	11. (400) [18.5] PF/	[3.] PF/	[1.] PF/	[20.] PF/	[3.] PF/	35. (2500) [36.] F/	[3.]	[6.]

Information Key:

Discharge Potential
in KVDC
(Discharge Current)
in 10^{-9} amps
[Breakdown Potential]
in KVDC

Notes: 1/, 2/, 3/, etc.

Notes:	
1/	gas conduction external to specimen
2/	column not powerable from start to 3000 hours
3/	column not powerable from 1500 to 3000 hours
4/	arcing external to specimen
F/	specimen failed
PF/	specimen failed previously

TABLE XI (Sheet 6 of 6)
RESULTS OF CORONA DISCHARGE AND BREAKDOWN TESTS

Material	Time (Hours)	Specimen Number 1	2	3	4	5	6	7	8	9	10
AA 620	100	27. 1/	↓								
↓	500	22. 1/	2/	23.5 1/							
↓	1500	20. 1/	↓	17. 1/	3/	3/	19. [19.] F/			3/	3/
↓	2050		↓		↓	↓		23. 1/		↓	↓
↓	3000	~20. [39.] 1/	~20. [38.] 1/	~20. [30.] 1/	~20. [42.] 1/	~20. [46.] 1/	[<1.]	~20. [30.] 1/	~20. [43.] 1/F/	[9.]	~20. [38.] 1/
↓	3000 @ 1 Atm	8. (2000) [50.] F/	29. (500) [62.] F/	27. (>2000) [41.] F/	16. (5000) [44.] F/	28. (1000) [56.] F/	[< 1.]	33. (2000) [44.] F/	[7.] F/	13. (1000) [49.] F/	17. (2000) [45.] F/

Information Key:

Discharge Potential
in KVDC
(Discharge Current)
in 10^{-9} amps
Breakdown Potential
in KVDC

Notes: 1/, 2/, 3/, etc.

Notes:
1/ gas conduction external to specimen
2/ column not powerable from start to 3000 hours
3/ column not powerable from 1500 to 3000 hours
4/ arcing external to specimen
F/ specimen failed
PF/ specimen failed previously

TABLE XII

VIBRATION TEST RESULTS

Compound Designation	Density (lbs/ft^3)	Resonant Frequency (cps)	Amplification at Resonant Freq.	Dwell Frequency (cps)	Amplification at Dwell Freq.	Stress at Dwell Freq. (psi)			Dwell Duration (Min.)			*Strength of Foam (psi)	
						20g	40g	60g	20g	40g	60g	Yield	Ultimate
AA-604	4	580	40	580	40	134	268	402	**	--	--	51	73
AA-608	8	1170	55	1170	55	184	368	552	**.25	--	--	128	159
AA-620	20	2600	70	200	1	3.3	6.7	10.0	15	15	15	894	1250
CPR 23-4	4	890	45	890	45	150	300	450	**	--	--	52	67
CPR 23-8	8	1200	35	1200	35	117	234	351	**8.5	--	--	173	230
CPR 23-20	20	2800	70	200	1	3.3	6.7	10.0	15	15	15	462	652

* From Table XIII

** Specimen failed at time indicated; when no time is indicated, failure occurred at start of dwell.

TABLE XIII
COMPRESSIVE STRENGTH TEST RESULTS

	STAFOAM						CPR					
	604		608		620		23-4		23-8		23-20	
	* //	** ⊥	//	⊥	//	⊥	//	⊥	//	⊥	//	⊥
Ultimate Compression Strength, psi	73	74	159	156	1250	1297	67	60	230	251	652	691
Compressive Yield Strength at 0.2% Offset, psi	51	50	128	125	894	1030	52	45	173	189	462	501
Modulus of Elasticity psi x 10^{-3}	16.8	18.5	40.2	42.8	140.2	166	7.6	10.0	26.2	27.0	70.0	74.8

* // = parallel to direction of foaming

** ⊥ = perpendicular to direction of foaming

TABLE XIV

RADIATION STABILITY TEST RESULTS

Specimen	Time (hrs)	Dielectric Constant	Dissipation Factor	Weight (grams)	Thickness (mils)	Diameter (inches)	Remarks
Stafoam AA 604	0	1.030	0.00105	1.275	251	1.995	White
	100	1.028	0.00095	1.254	251	1.995	Tan exposed surface
	350	1.020	0.00091	1.248	251	1.987	Tan exposed surface
	850	1.022	0.00095	1.253	251	1.986	Surface light brown
	1350	1.022	0.00114	1.250	251	1.987	Surface brown
	1850	1.022	0.00095	1.250	251	1.991	No further change
	2375	1.018	0.00085	1.244	252	1.991	No further change
	3048	1.015	0.0012	1.243	248	1.991	No further change
Stafoam AA 608	0	1.042	0.00172	2.120	252	1.995	White
	100	1.040	0.00140	2.092	252	1.995	Tan exposed surface
	350	1.038	0.00136	2.085	252	1.990	Tan exposed surface
	850	1.040	0.00140	2.091	252	1.987	Surface light brown
	1350	1.048	0.00168	2.091	252	1.989	Surface brown
	1850	1.042	0.00144	2.087	252	1.985	No further change
	2375	1.035	0.00124	2.079	252	1.985	No further change
	3048	1.043	0.00096	2.078	250	1.983	No further change
Stafoam AA 620	0	1.106	0.00250	5.169	251	1.994	White
	100	1.098	0.00182	5.108	252	1.994	Tan exposed surface
	350	1.096	0.00168	5.080	251	1.990	Tan exposed surface
	850	1.100	0.00186	5.077	252	1.989	Surface light brown
	1350	1.098	0.00199	5.075	252	1.987	Surface brown
	1850	1.100	0.00185	5.074	251	1.987	No further change
	2375	1.118	0.00183	5.069	253	1.986	No further change
	3048	1.093	0.00156	5.067	251	1.989	No further change
CPR 23-4	0	1.036	0.00151	1.521	252	1.995	White
	100	1.028	0.00132	1.493	251	1.995	Tan exposed surface
	350	1.026	0.00128	1.485	251	1.989	Tan exposed surface
	850	1.030	0.00132	1.493	251	1.987	Surface light brown
	1350	1.028	0.00175	1.488	251	1.985	Surface brown
	1850	1.022	0.00133	1.488	252	1.986	No further change
	2375	1.030	0.00111	1.478	253	1.987	No further change
	3048	1.033	0.00073	1.478	250	1.983	No further change
CPR23-8	0	1.048	0.00204	2.387	251	1.995	White
	100	1.044	0.00151	2.341	250	1.994	Tan exposed surface
	350	1.042	0.00149	2.334	250	1.991	Tan exposed surface
	850	1.048	0.00154	2.342	250	1.988	Surface light brown
	1350	1.044	0.00167	2.338	250	1.989	Surface brown
	1850	1.045	0.00139	2.338	250	1.987	No further change
	2375	1.078	0.00128	2.328	251	1.987	No further change
	3048	1.045	0.00101	2.327	249	1.985	No further change
CPR23-20	0	1.088	0.00317	4.156	252	1.995	White
	100	1.080	0.00212	4.070	251	1.994	Tan exposed surface
	350	1.084	0.00214	4.059	251	1.990	Tan exposed surface
	850	1.080	0.00226	4.064	251	1.987	Surface light brown
	1350	1.080	0.00244	4.061	251	1.988	Surface brown
	1850	1.081	0.00215	4.060	251	1.987	No further change
	2375	1.114	0.00199	4.050	253	1.987	No further change
	3048	1.084	0.00177	4.050	251	1.985	No further change

TABLE XV

THERMAL IMPEDANCE TEST RESULTS

Foam	*Therm No.	**1 watt-10%		1 watt-25%		2 watt-10%		2 watt-25%		5 watt-10%		5 watt-25%		10 watt-10%		10 watt-25%	
		RT	80°C	RT	80°C	RT	80°C	RT	80°C	RT	80°C	RT	80°C	RT	80°C	RT	80°C
604	1	95°F	194°F	131°F	224°F	110°F	203°F	165°F	250°F	160°F	257°F	278°F	368°F	227°F	314°F	408°F	488°F
	2	84	182	100	196	90	189	120	210	115	214	170	304	146	244	256	348
	3	80	180	94	190	84	183	103	194	100	204	[illegible]	243	121	220	192	286
	4	78	179	88	184	76	178	84	180	78	185	[illegible]	196	84	188	106	209
608	1	94	193	126	220	110	208	164	255	196	292	362	339	228	315	406	495
	2	82	182	97	194	88	188	110	208	122	224	199	296	153	252	262	368
	3	79	180	91	189	83	184	100	198	111	214	166	[illegible]	124	open	196	301
	4	74	178	80	180	74	177	80	180	84	192	106	214	89	195	110	218
620	1	91	190	122	217	107	203	157	249	138	239	236	314	199	296	386	471
	2	80	180	96	194	88	188	108	206	105	208	254	250	140	238	241	329
	3	80	180	92	191	84	184	100	198	97	200	132	230	126	226	208	298
	4	78	178	86	185	80	181	88	189	88	194	110	212	108	226	160	255
23-4	1	96	195	131	226	110	208	166	255	160	260	288	394	231	320	410	488
	2	82	182	96	195	91	190	116	211	115	219	181	280	160	256	282	379
	3	78	180	88	188	85	185	105	200	102	207	148	250	132	230	218	315
	4	74	176	79	180	76	177	82	181	88	190	94	207	108	210	158	258
23-8	1	93	191	125	221	109	204	160	248	202	296	380	450	221	320	407	490
	2	81	180	94	193	90	188	116	206	120	221	197	287	141	245	240	343
	3	80	178	90	188	86	184	107	198	106	207	161	253	118	224	186	288
	4	77	176	84	182	82	180	97	188	84	189	104	205	82	189	92	205
23-20	1	92	192	122	220	105	204	153	245	155	253	278	366	198	296	382	470
	2	80	182	94	193	88	188	110	206	103	205	154	245	130	232	218	315
	3	79	180	88	188	84	184	101	197	96	199	136	228	119	222	170	290
	4	76	178	81	182	80	181	94	189	82	193	120	212	93	198	125	225

* Thermocouple Number (see figure
No. 1 On resistor body
No. 2 1/2" from resistor
No. 3 1" from resistor
No. 4 Specimen surface (2" from resistor)

** Power Rating of Resistor and Percent of Power Rating at which Operated.

*** Ambient Temperature
RT - Room Temperature

VII. Illustrations

VII. Illustrations (continued)

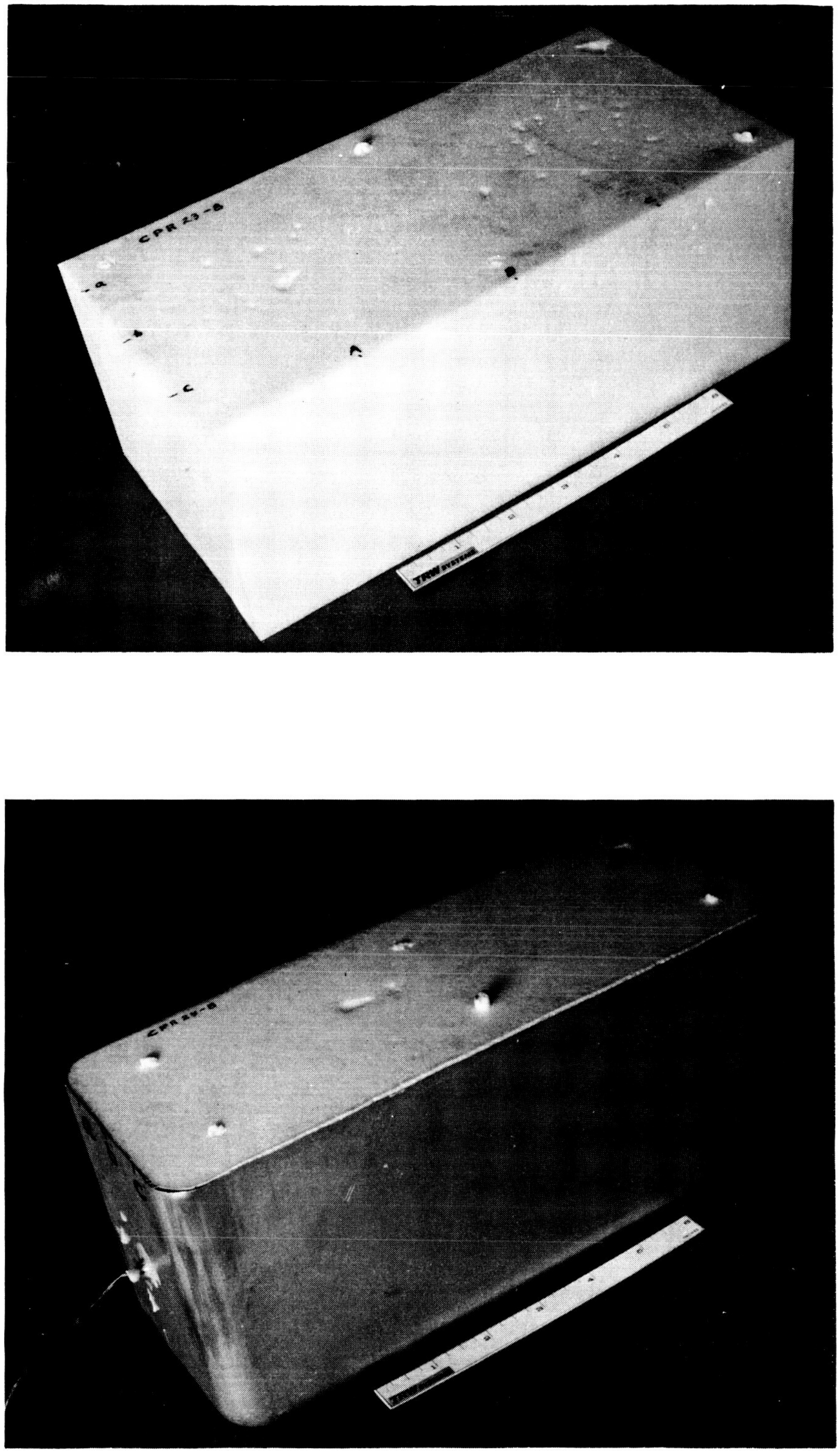

Figure 1

TYPICAL THERMAL AGING SPECIMENS

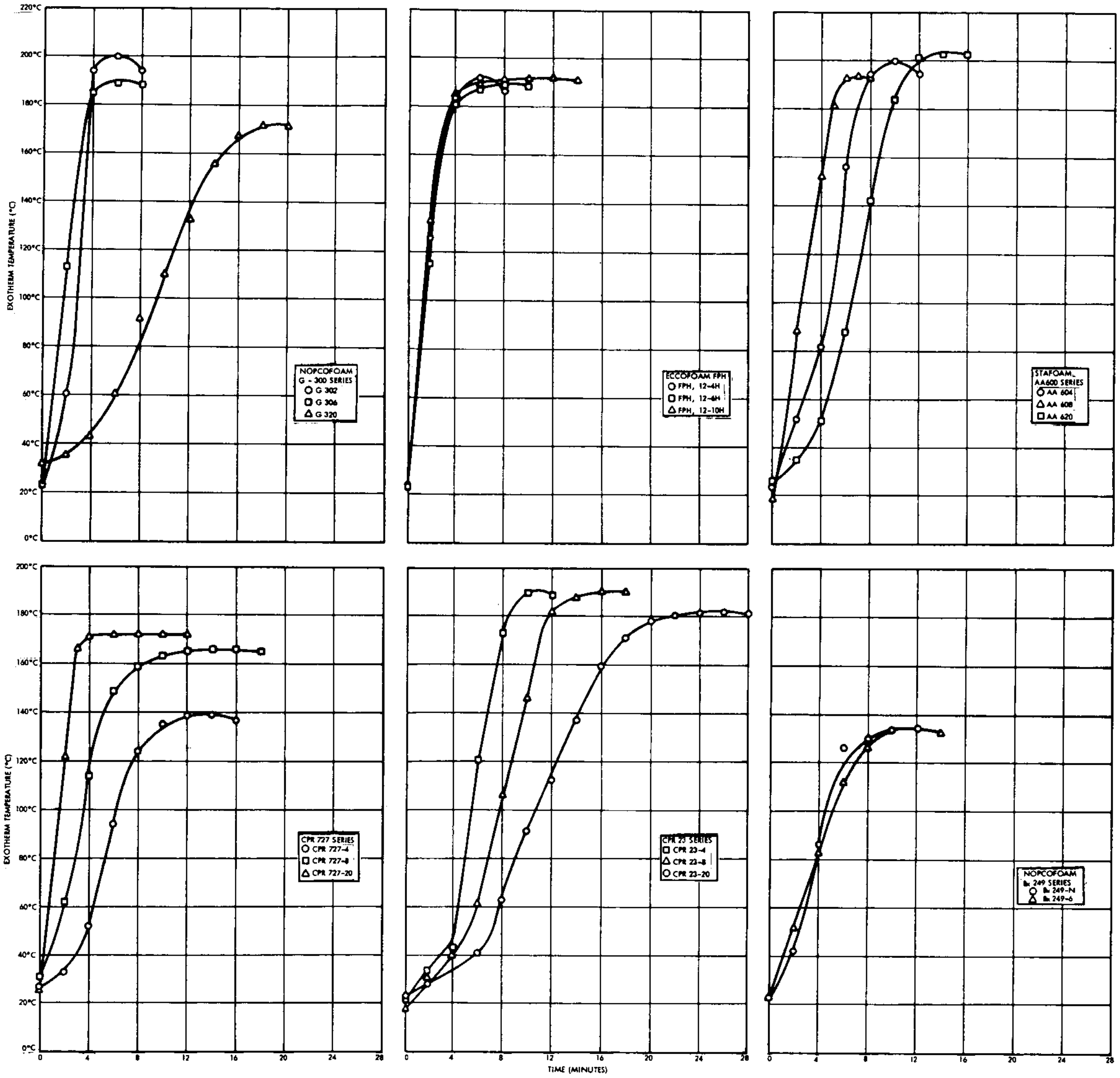

Figure 2

COMPOUND EXOTHERM TEMPERATURES

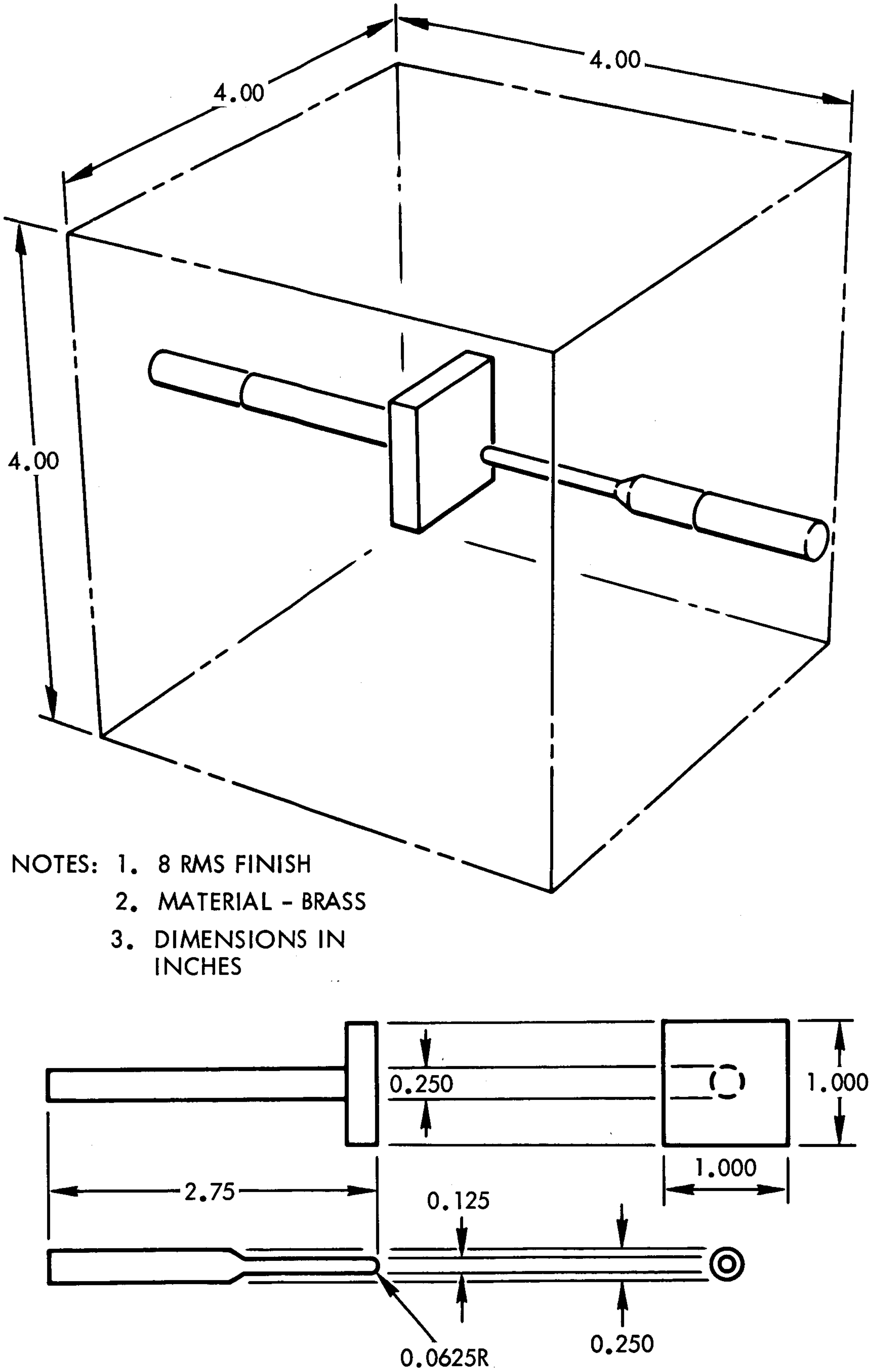

NOTES: 1. 8 RMS FINISH
2. MATERIAL - BRASS
3. DIMENSIONS IN INCHES

Figure 3

DIELECTRIC SPECIMEN AND ELECTRODE CONFIGURATION

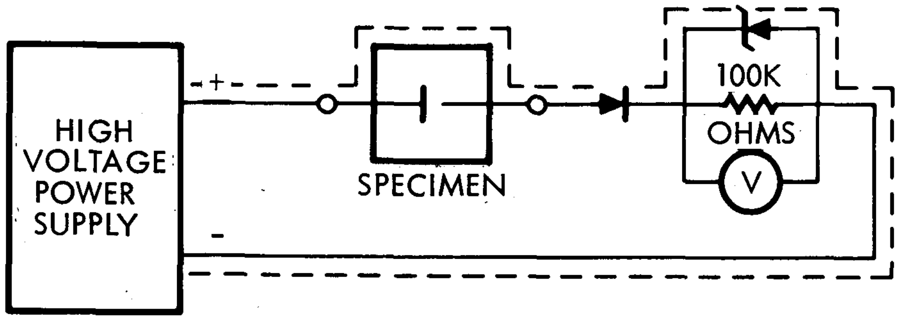

Figure 4

ELECTRICAL CIRCUIT FOR CORONA AND BREAKDOWN VOLTAGE TEST

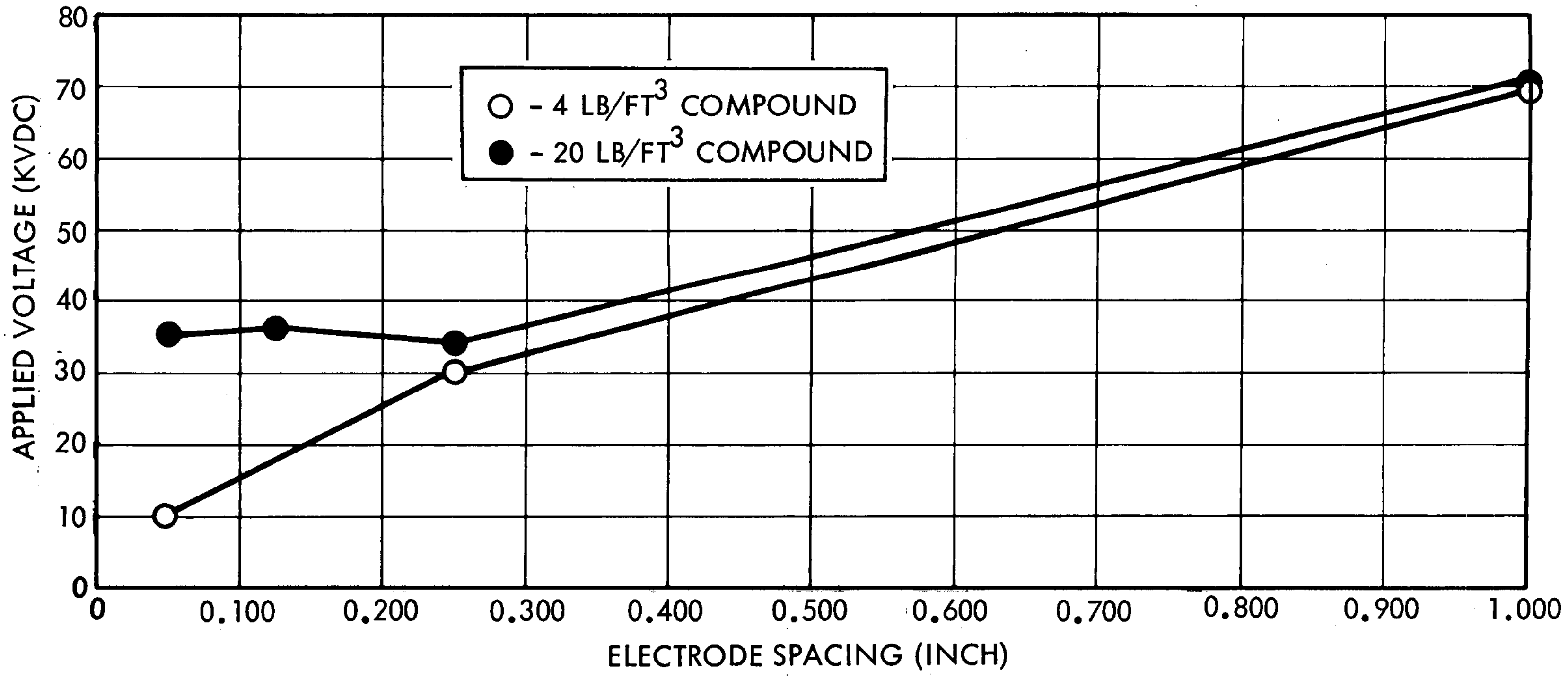

Figure 5

CORONA DISCHARGE POTENTIAL AS A FUNCTION
OF ELECTRODE SPACING

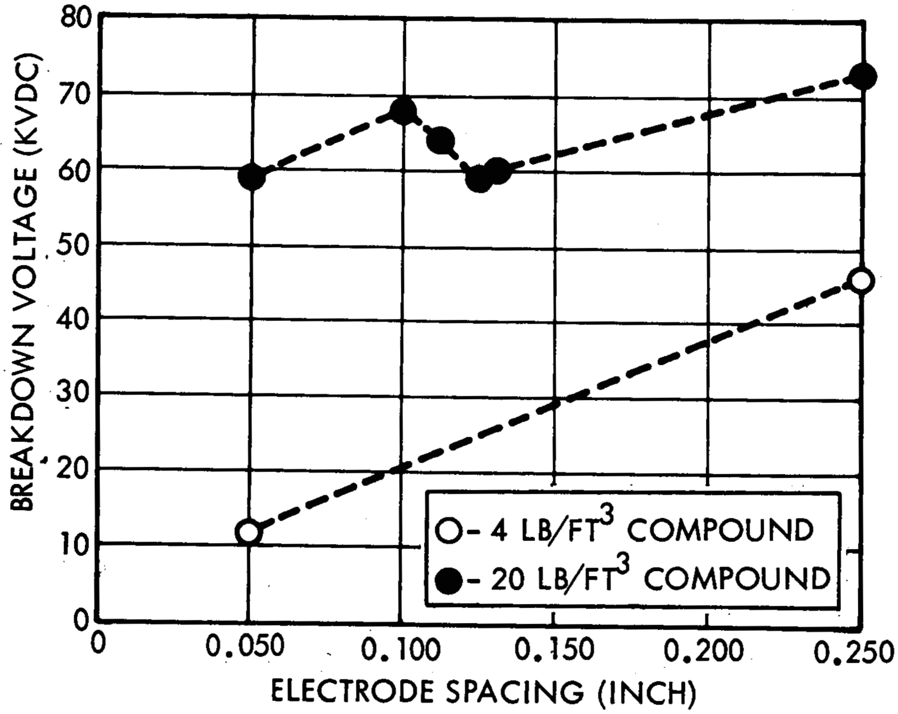

Figure 6

BREAKDOWN POTENTIAL AS A
FUNCTION OF ELECTRODE SPACING

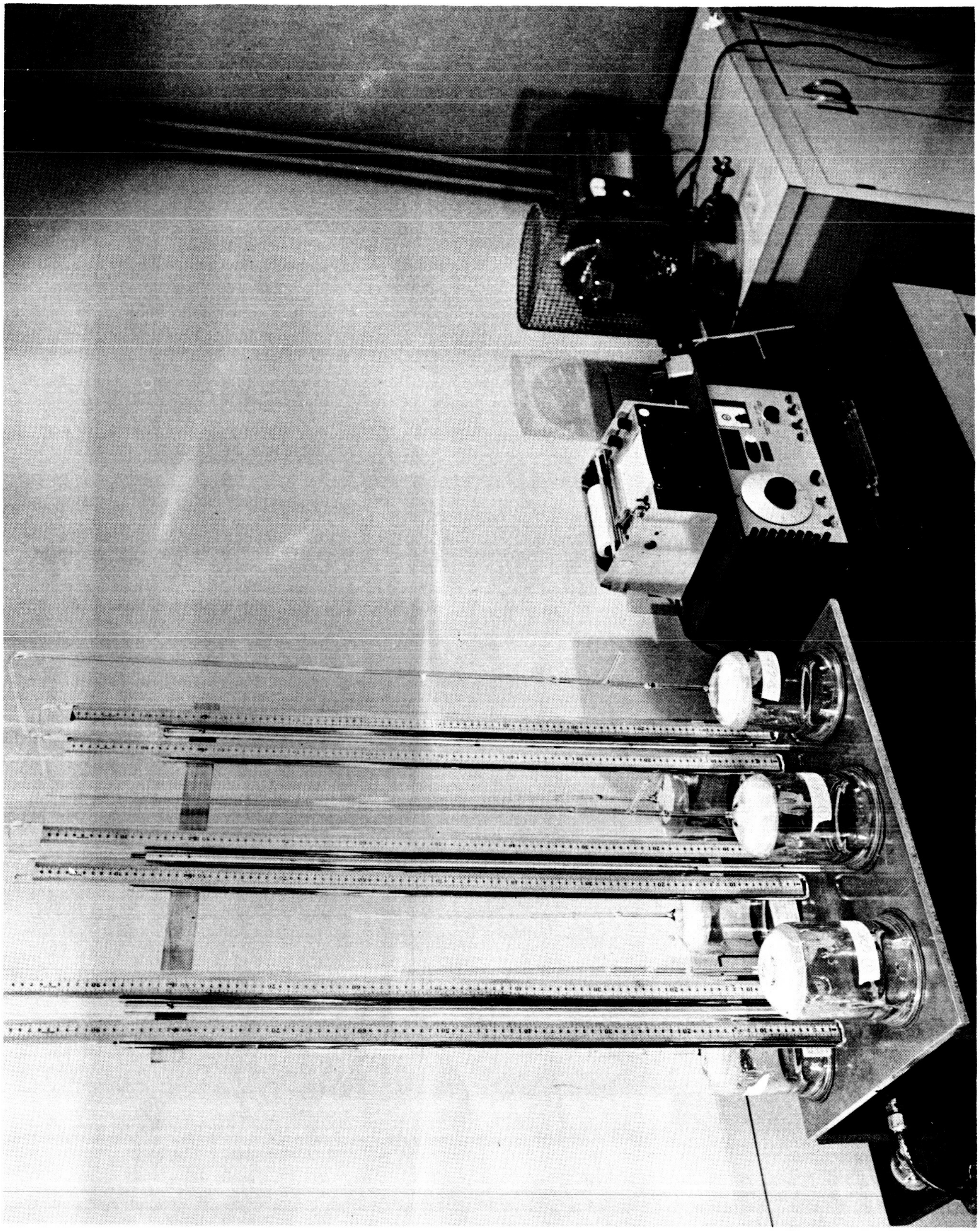

Figure 7

GAS PERMEABILITY APPARATUS

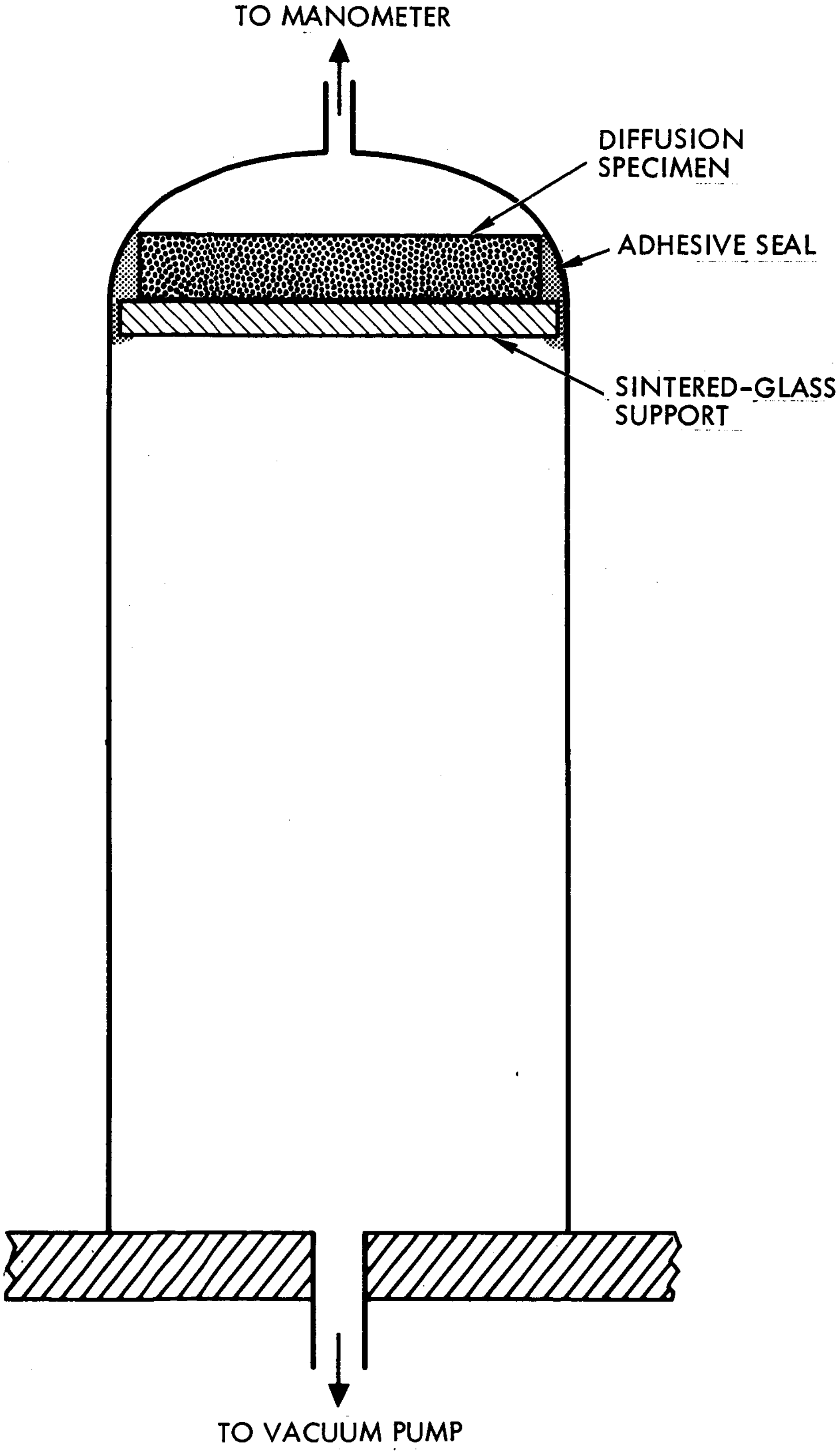

Figure 8

GAS DIFFUSION RATE TEST SPECIMEN

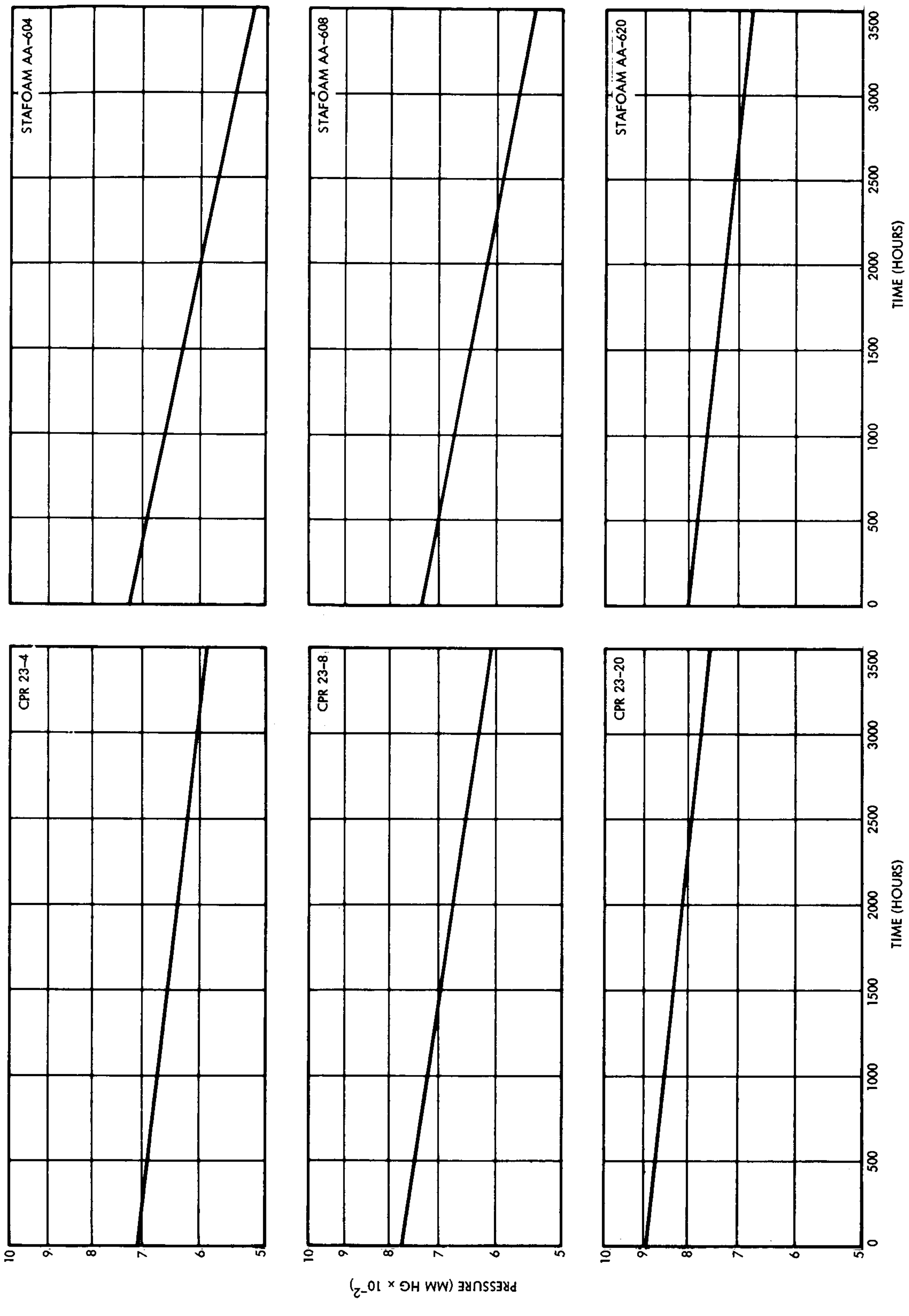

Figure 9

PERMEABILITY TEST RESULTS

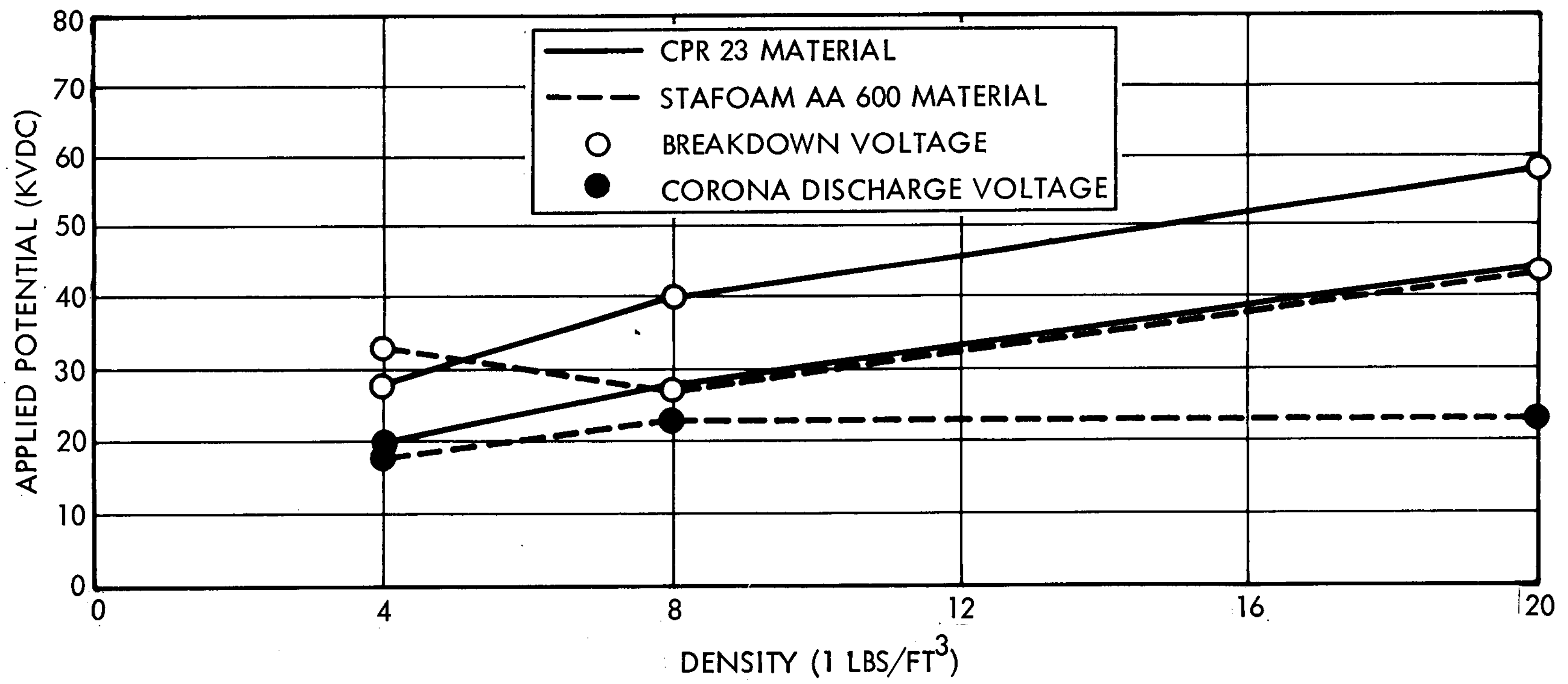

Figure 10

SUMMARY OF VACUUM - DIELECTRIC TEST

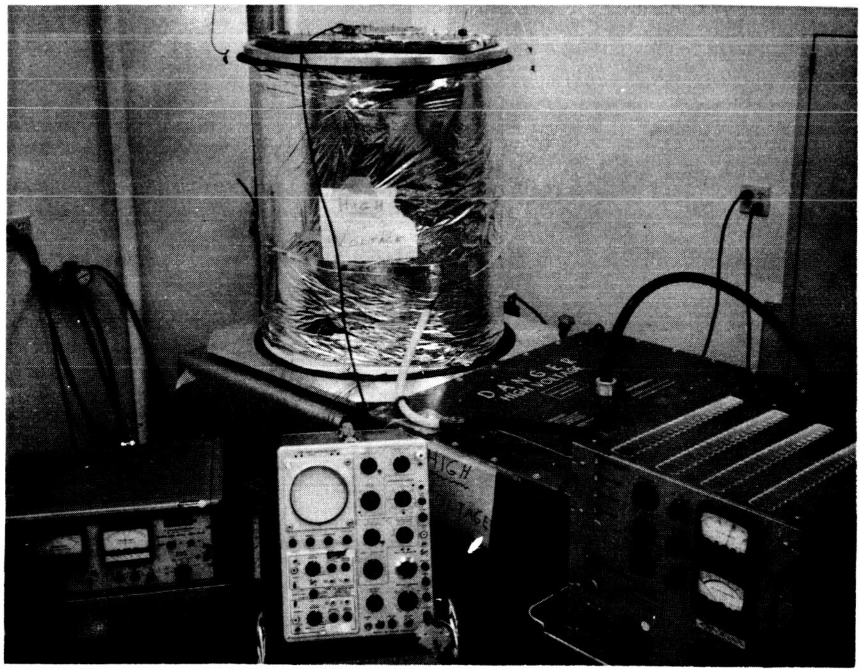

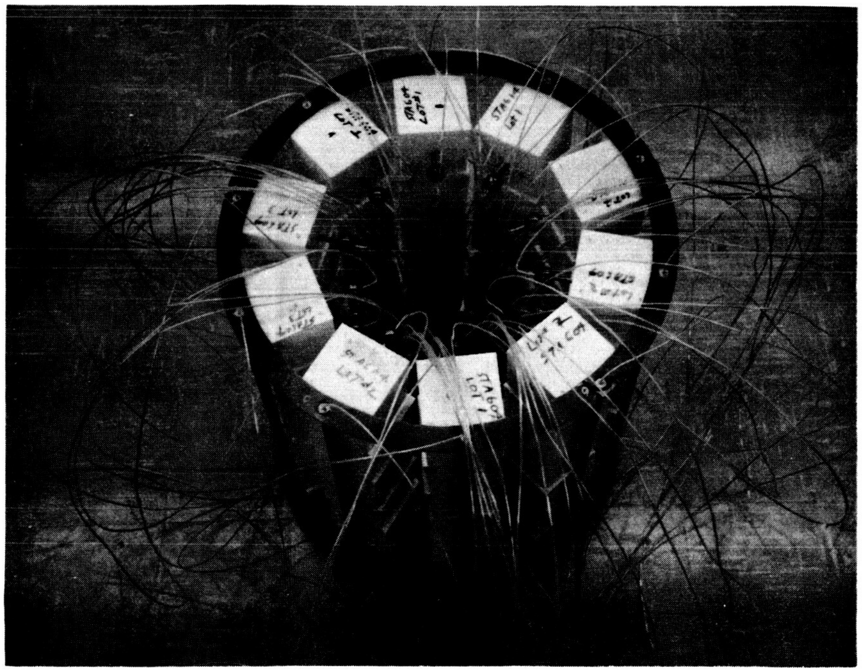

TOP: Vacuum Dielectric Test Apparatus
BOTTOM: Specimen Arrangement and Support Structure

Figure 11

VACUUM-DIELECTRIC TEST SET-UP

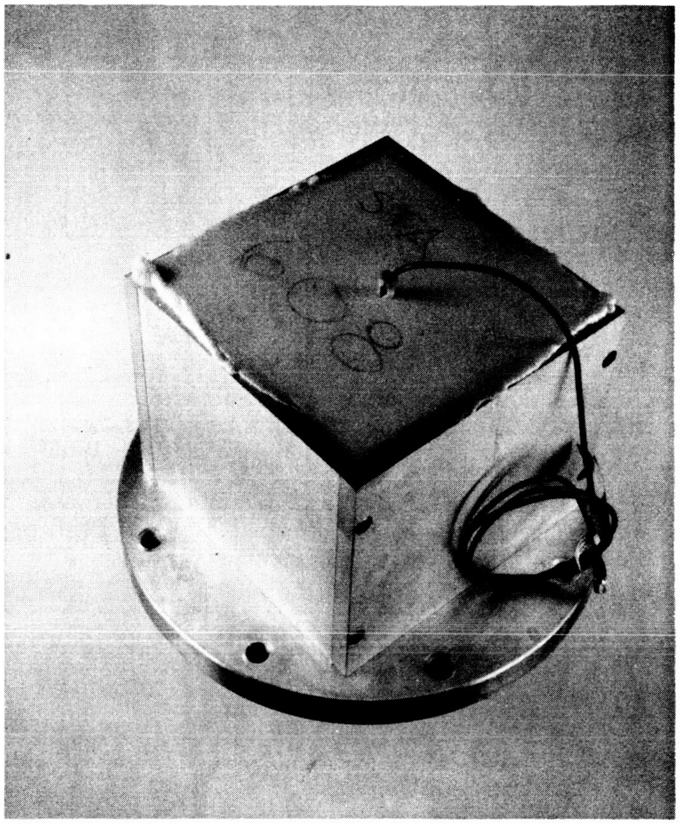

Figure 12

TYPICAL VIBRATION TEST SPECIMEN

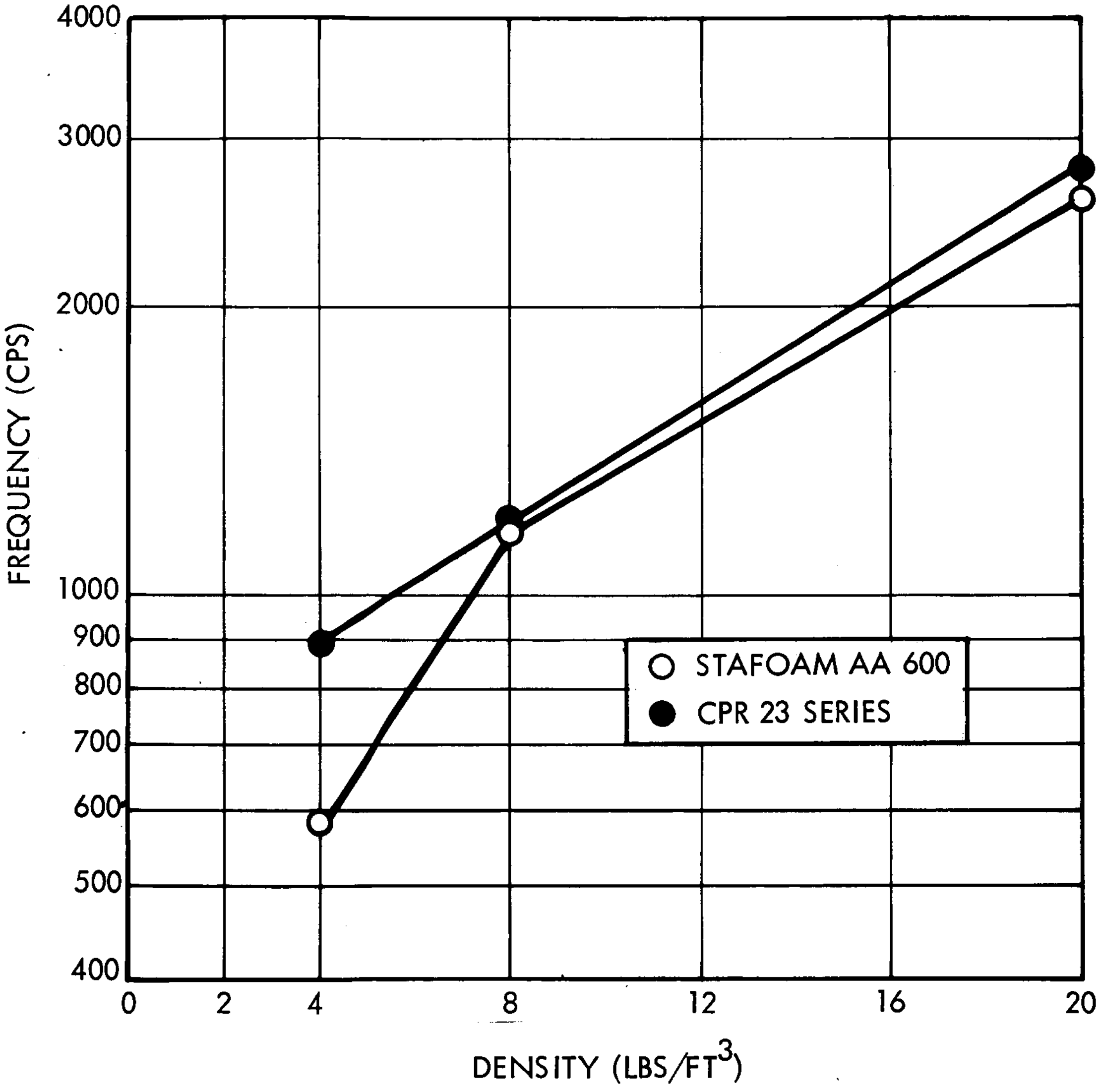

Figure 13

VIBRATION TEST RESULTS

RESONANT FREQUENCY AS A FUNCTION OF DENSITY

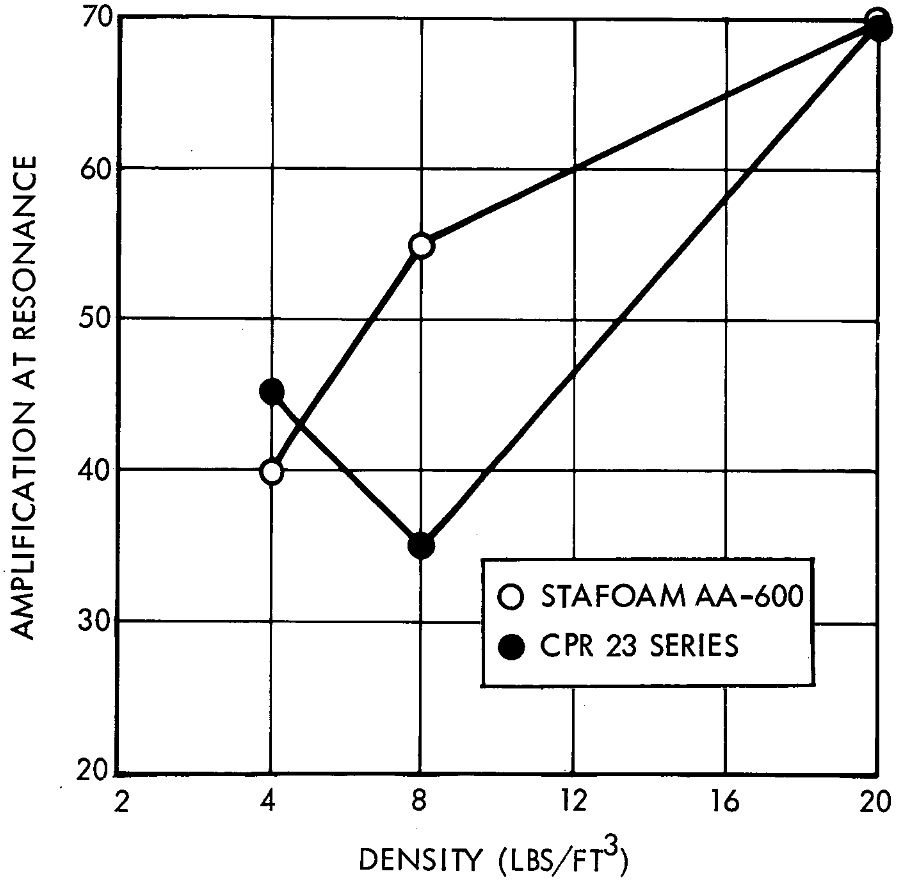

Figure 14

VIBRATION TEST RESULTS
DENSITY VS AMPLIFICATION AT RESONANCE

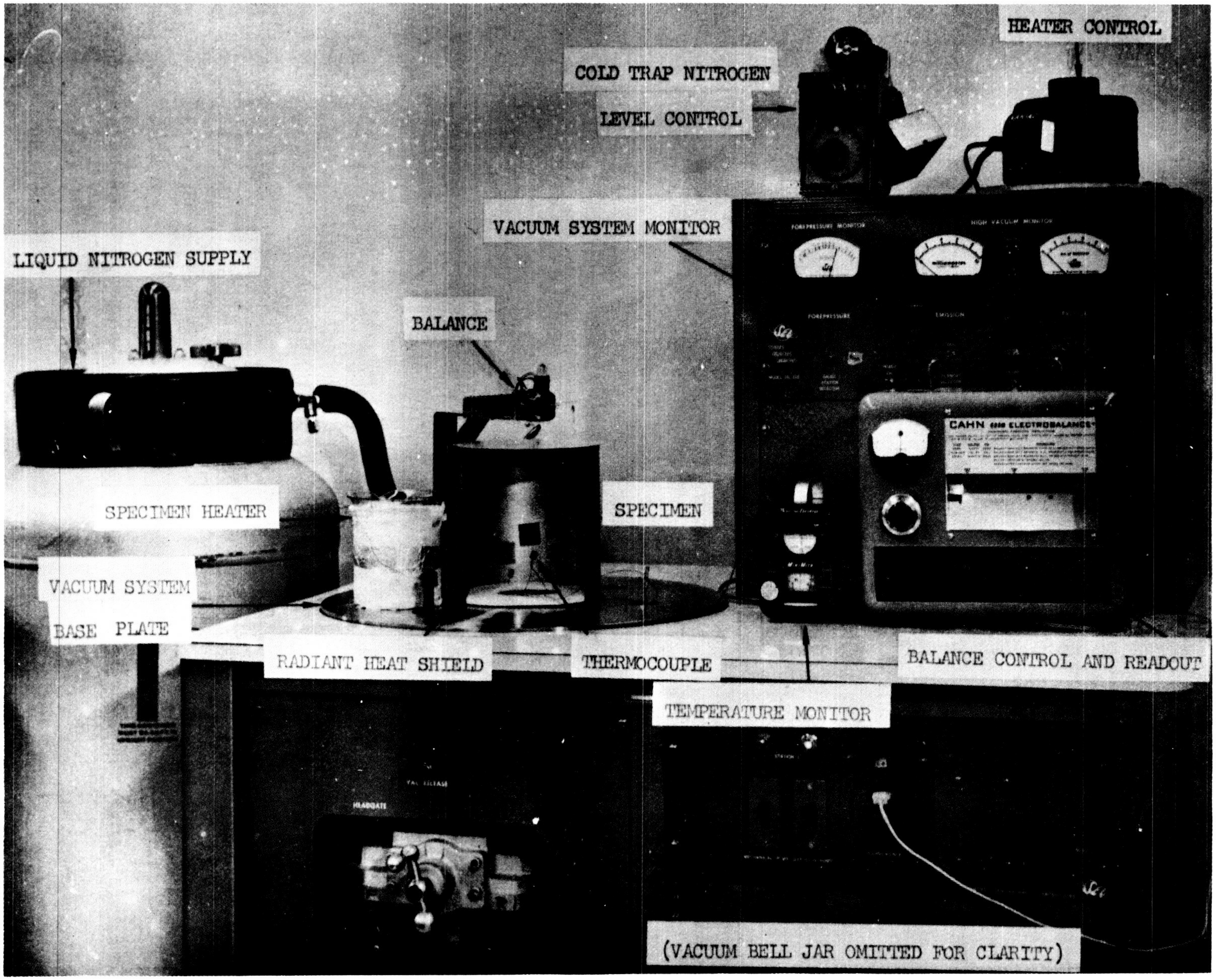

Figure 15
PHOTOGRAPH OF VACUUM WEIGHT LOSS APPARATUS

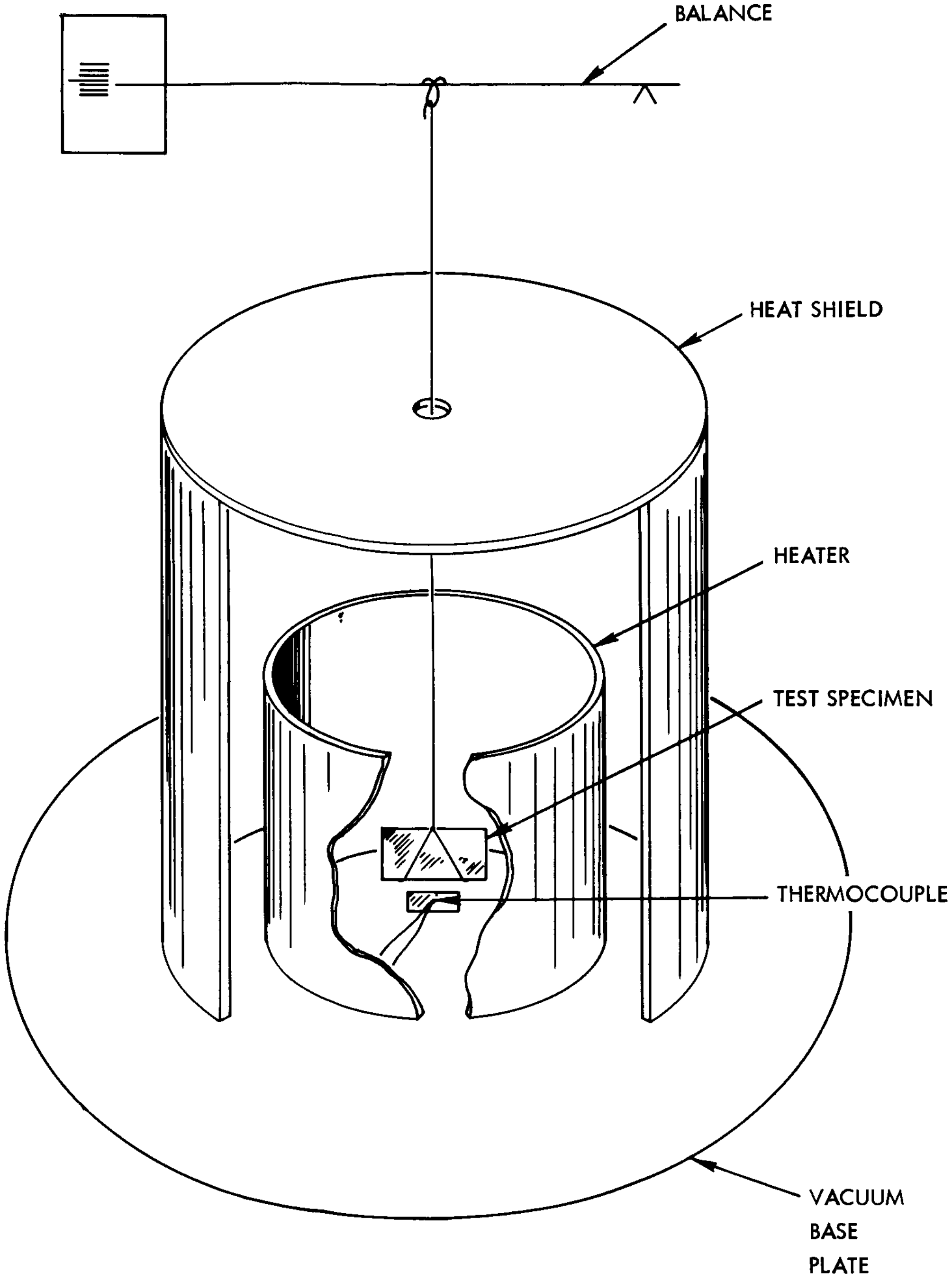

Figure 16

SCHEMATIC OF EXPERIMENTAL APPARATUS
USED IN SUBLIMATION STUDY

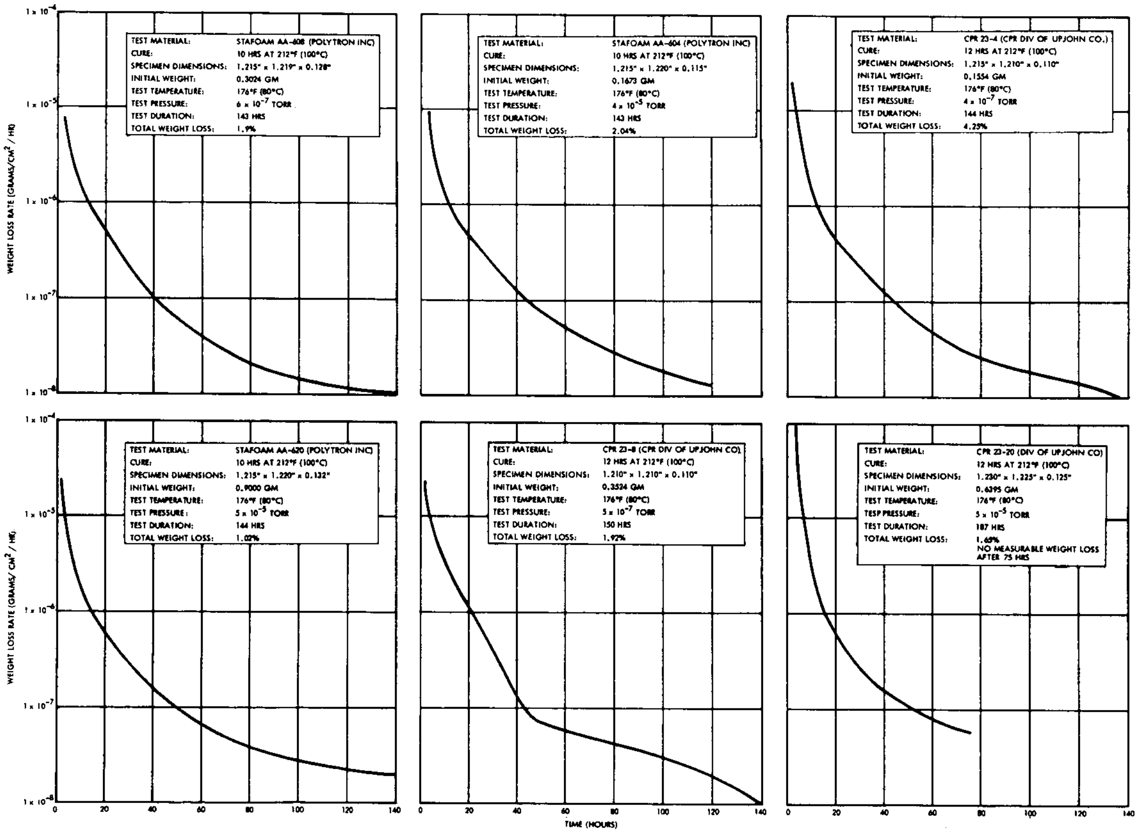

Figure 17

VACUUM WEIGHT LOSS RESULTS

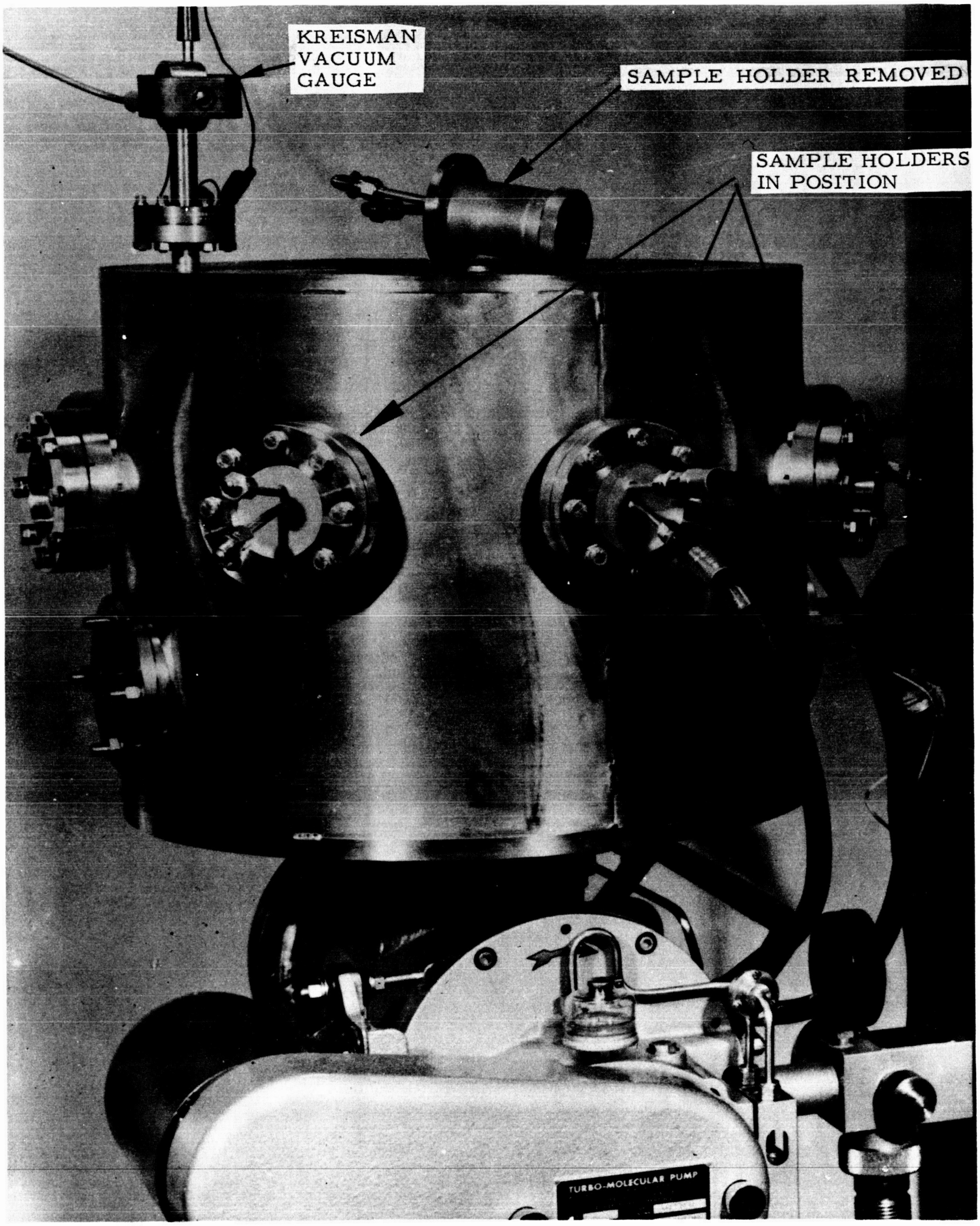

Figure 18

TURBO MOLECULAR PUMPED ULTRAVIOLET DEGRADATION CHAMBER

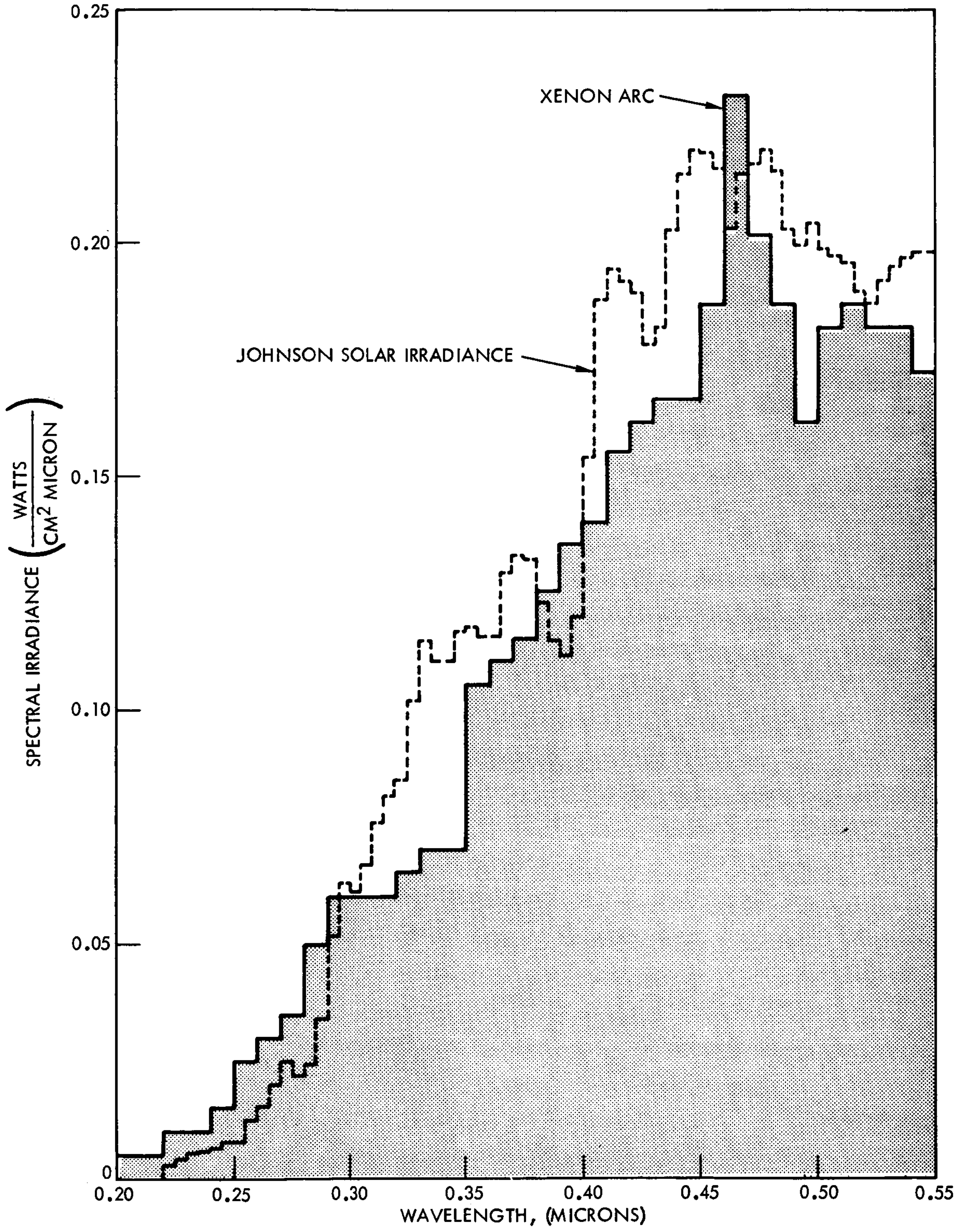

Figure 19

SPECTRAL ENERGY DISTRIBUTION OF XENON ARC
COMPARED WITH JOHNSON[4] SOLAR SPECTRUM

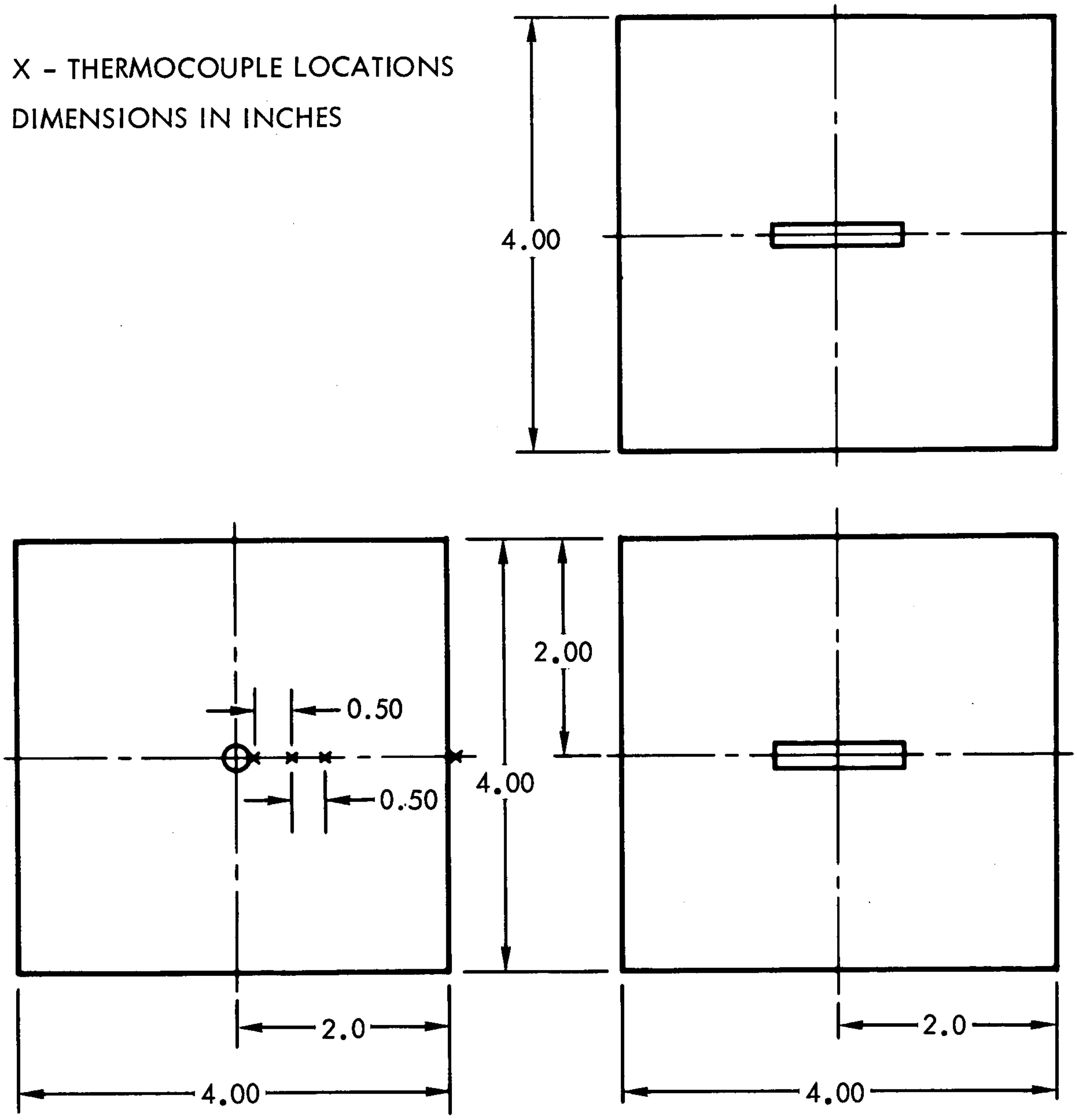

Figure 20

SPECIMEN CONFIGURATION - THERMAL IMPEDANCE TEST

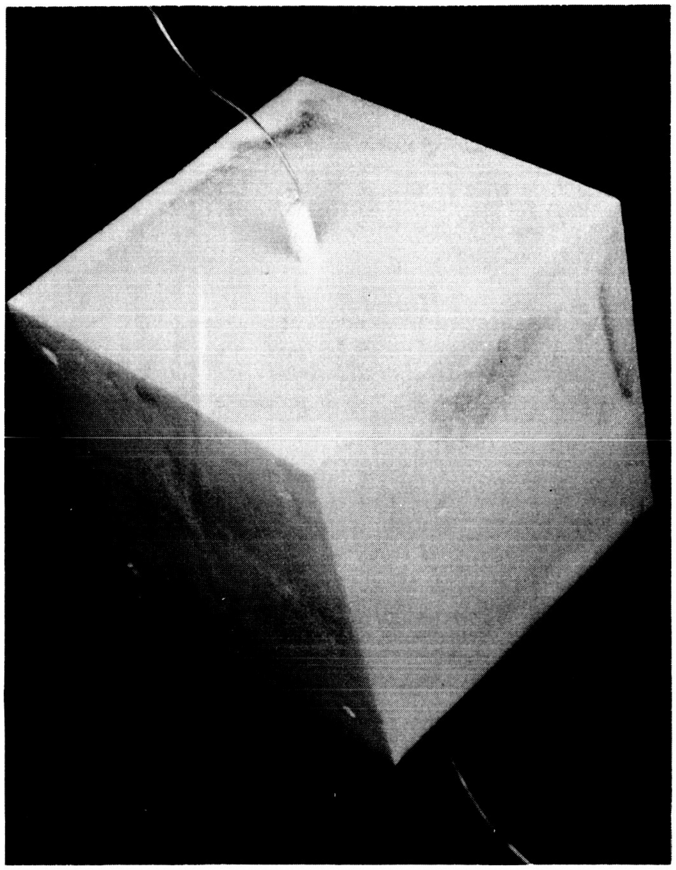

Figure 21

PHOTOGRAPH OF THERMAL IMPEDANCE
TEST SPECIMEN

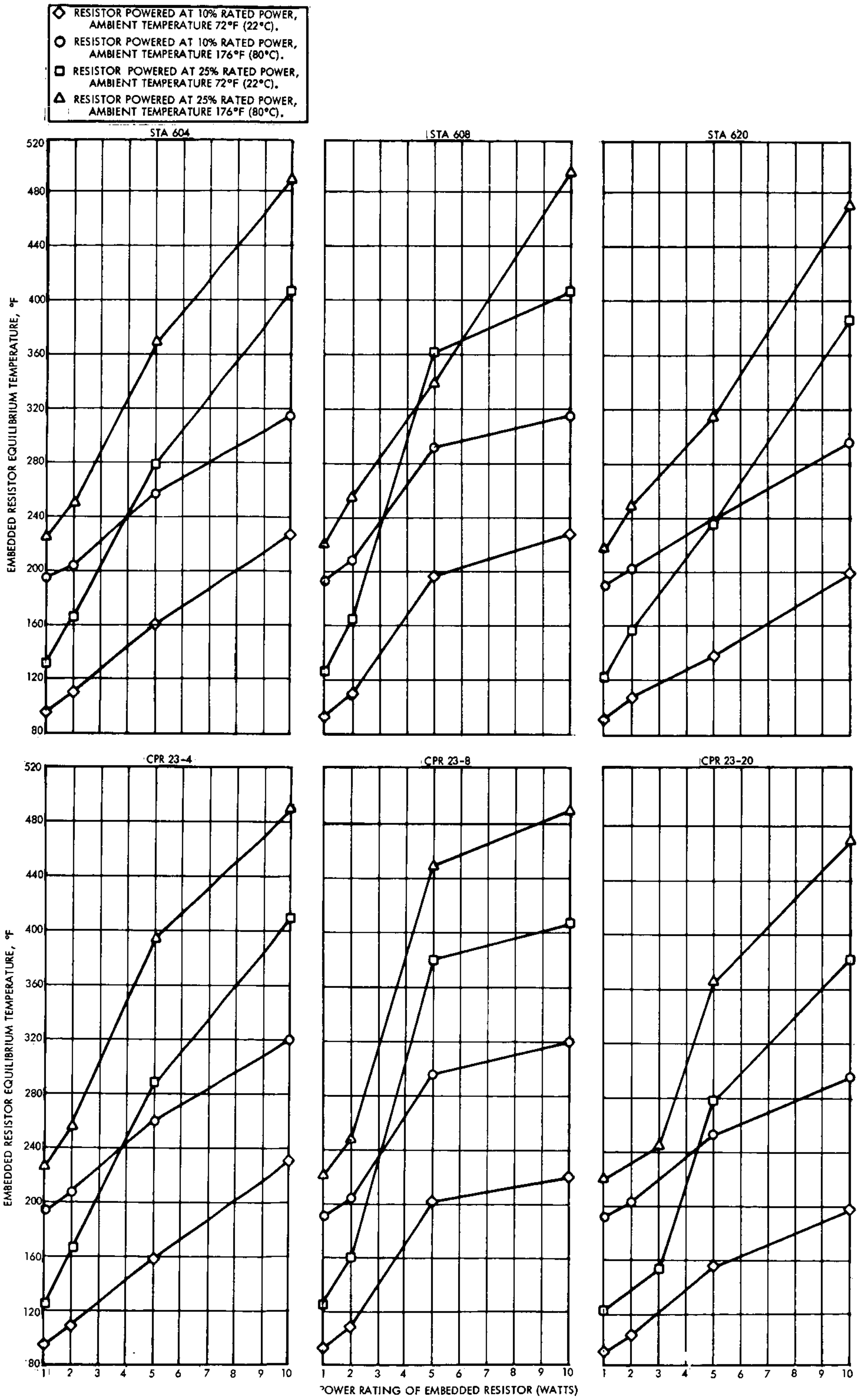

Figure 22

THERMAL IMPEDANCE TEST RESULTS

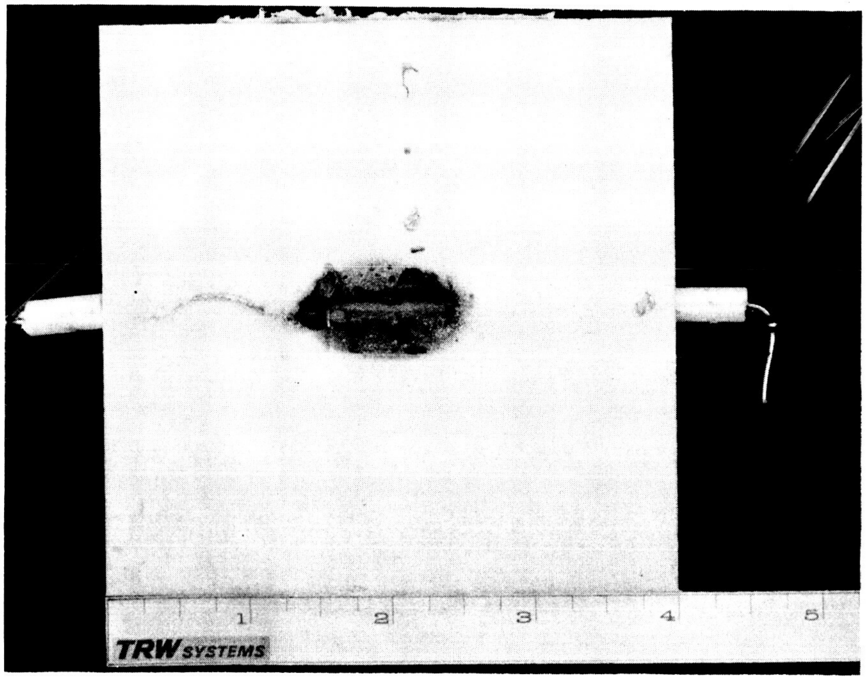

Magnification .75X

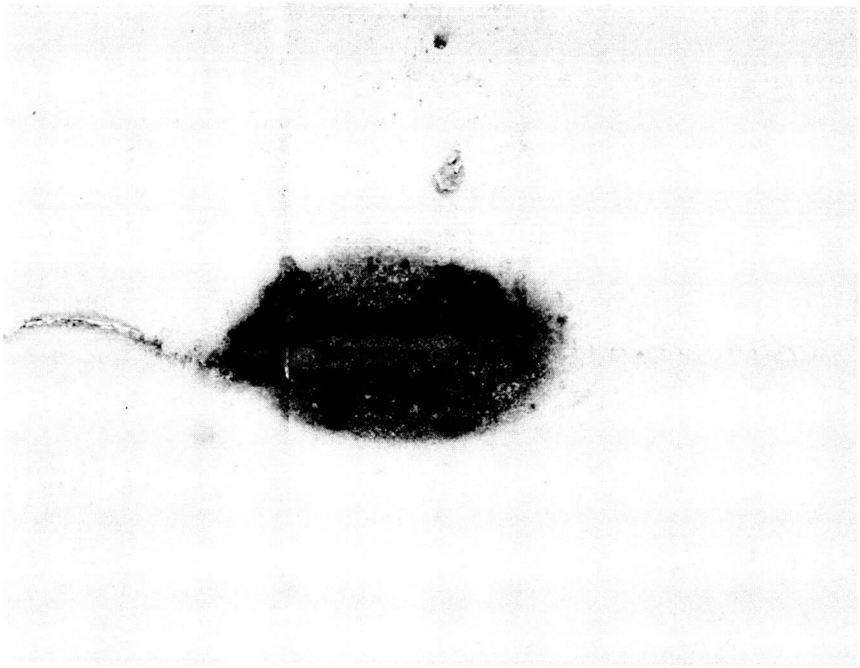

Magnification 1.5X

Figure 23

TYPICAL DEGRADATION OF 5-WATT RESISTOR SPECIMENS

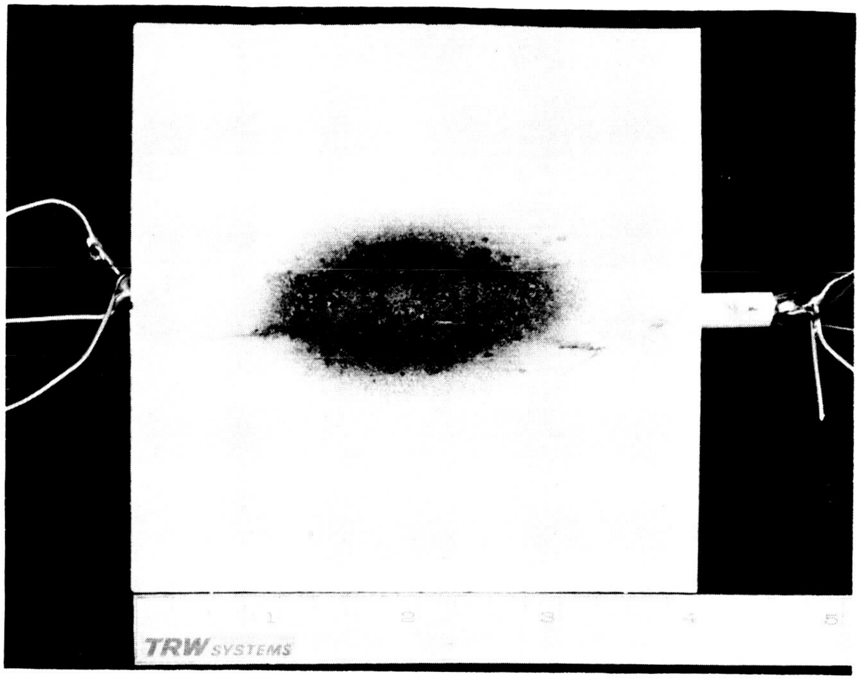

Magnification .75X

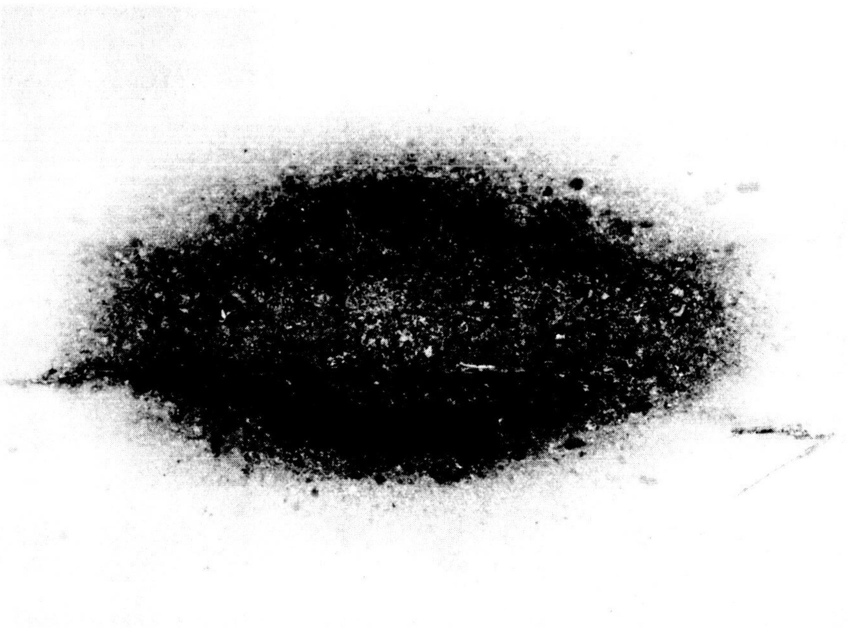

Magnification 1.5X

Figure 24

TYPICAL DEGRADATION OF 10-WATT RESISTOR SPECIMENS